JOC The Journal of Organic Chemistry

Article

pubs.acs.org/joc

Near-IR Emissive Chlorin–Bacteriochlorin Energy-Transfer Dyads with a Common Donor and Acceptors with Tunable Emission Wavelength

Zhanqian Yu and Marcin Ptaszek*

Department of Chemistry and Biochemistry, University of Maryland, Baltimore County, 1000 Hilltop Circle, Baltimore, Maryland 21250, United States

Supporting Information

ABSTRACT: Design, synthesis, and optical properties of a series of novel chlorin–bacteriochlorin energy transfer dyads are described. Each dyad is composed of a common red-absorbing (645–646 nm) chlorin, as an energy donor, and a different near-IR emitting bacteriochlorin, as an energy acceptor. Each bacteriochlorin acceptor is equipped with a different set of auxochromes, so that each of them emits at a different wavelength. Dyads exhibit an efficient energy transfer (≥0.77) even for chlorin–bacteriochlorin pairs with large (up to 122 nm) separation between donor emission and acceptor absorption. Excitation of the chlorin donor results in relatively strong emission of the bacteriochlorin acceptor, with a quantum yield Φ_f range of 0.155–0.23 in toluene and 0.12–0.185 in DMF. The narrow, tunable emission band of bacteriochlorins enables the selection of a series of three dyads with well-resolved emissions at 732, 760, and 788 nm, and common excitation at 645 nm. Selected dyads have been also converted into bioconjugatable *N*-succinamide ester derivatives. The optical properties of the described dyads make them promising candidates for development of a family of near-IR fluorophores for simultaneous imaging of multiple targets, where the whole set of fluorophores can be excited with the common wavelength, and fluorescence from each can be independently detected.

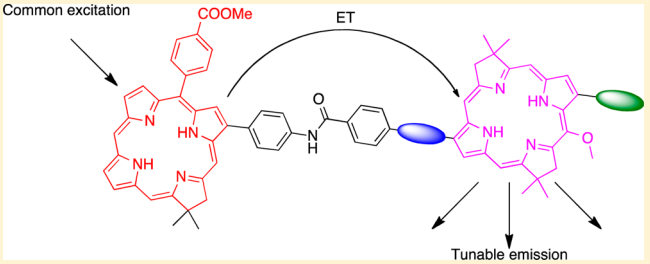

INTRODUCTION

Multicolor in vivo fluorescence imaging has recently emerged as a promising tool for medicinal diagnosis of various diseases, by the capability for simultaneous visualization of multiple disease markers, multiple cells, or multiple pathological processes.[1−10] Multicolor imaging utilizes a set of fluorophores, with distinct emission bands, and differentiation between fluorophores is achieved by independent fluorescence detection from each individual fluorophore. Ideally, fluorophores for multicolor imaging should exhibit distinct, well-resolved emission bands, so that emission of each individual fluorescent probe can be selectively detected in the presence of other probes. Additionally, the capability to excite the whole set of fluorophores with a common wavelength is highly beneficial for practical applications, because this simplifies and speeds the imaging process.[3] In practice, these requirements are difficult to achieve for fluorophores suitable for in vivo imaging. For deep tissue applications, fluorophores should absorb and emit in the red or near-IR spectral window (650–900 nm) where light has the deepest tissue penetration, and light scattering and tissue autofluorescence are diminished.[1,2] Several classes of fluorophores have been exploited for in vivo multicolor imaging, including small organic molecules,[4−7] fluorescent proteins,[8] quantum dots,[3] upconverting nanocrystals,[9] and upconverting nanocrystal–organic fluorophore conjugates.[10] Because of the broad emission bands (∼40 nm and more) of typical organic fluorophores used in the red and near-IR regions (e.g., cyanine dyes),[11] the number of fluorophores that can be simultaneously used in this narrow spectral window is limited. The same organic fluorophores typically also have narrow excitation bands, with a relatively small Stokes shift.[11] Both of these features make the efficient excitation of a whole set of fluorophores, emitting at different wavelengths, with a single wavelength challenging, if possible at all. Therefore, application of organic fluorophores for in vivo imaging requires multiple cycles of excitation and detection,[4,5] which is technically demanding and limits the temporal resolution of the imaging. Alternatively, quantum dots, which exhibit broad absorption band and tunable, narrow emission can be excited simultaneously in vivo at a common wavelength and used for multicolor imaging;[3] however, their potential toxicity raises a concern for use for humans.[12]

Development of improved sets of fluorophores for multicolor imaging would therefore require overcoming two major limitations of organic fluorophores: their broad emission spectra (which limits the number of fluorophores available for simultaneous use) and narrow, distinctive excitation bands (which imposes a necessity for multiple excitation cycles).

Received: August 1, 2013
Published: September 30, 2013

Chlorins and bacteriochlorins (collectively termed hydroporphyrins) are the tetrapyrrolic macrocycles which constitute the core of naturally occurring photosynthetic pigments: chlorophylls and bacteriochlorophylls.[13] Synthetic and semisynthetic hydroporphyrins possess a set of unique properties, which makes them particularly well-suited for development of fluorophores for multicolor in vivo imaging. They strongly absorb and emit in the red (chlorins, 600−700 nm) and near-IR (bacteriochlorins, 710−823 nm) spectral window and exhibit appreciable fluorescence quantum yields (chlorins 0.20−0.40, bacteriochlorins 0.10−0.25).[14−20] Both chlorins and bacteriochlorins have already been examined for in vivo fluorescence imaging.[21,22] Hydroporphyrins have also been proposed for use as contrast agents for in vivo photoacoustic cancer imaging.[23] Another attractive feature of hydroporphyrins is the possibility of combining imaging modality with therapeutic capability, that is, with singlet oxygen photosensitization for photodynamic therapy[22] or with photothermal therapy.[23]

Hydroporphyrins exhibit exceptionally narrow emission bands among organic compounds. Typically, the full width at half maximum (fwhm) for emission bands is ∼12−19 nm for chlorins,[24] and 12−25 nm for bacteriochlorins.[15,17] Consequently, emission bands in hydroporphyrins are narrower than in the cases of other near-IR fluorophores used in bioimaging, such as cyanine dyes or quantum dots.[11,17] Moreover, the position of long-wavelength absorption and emission bands can be adjusted with high precision, by a relatively simple substitution on the pyrrole rings, i.e., the 3- and 13-positions of the macrocycle (for numbering of chlorins and bacteriochlorins, see Figure 1).[15−19] Taken together, it is possible to select a series of chlorin and bacteriochlorin derivatives spanning the spectral window of ∼650−820 nm, with minimally overlapped emission bands, with maxima separated by ∼25 nm.[15,17,19] However, because hydroporphyrins exhibit narrow excitation bands in the near-IR spectral window (fwhm typically closely matches their emission bands) and a small Stokes shift (typically ≤10 nm),[15,19] they still require a separate excitation wavelength for each derivative. The possible solution for that is to incorporate hydroporphyrins into energy transfer (ET) dyads. ET dyads[25,26] are composed of a donor and an acceptor, and excitation of the donor results in the transfer of excitation energy to an acceptor and, consequently, acceptor emission. If quantum efficiency of energy transfer is high enough, an ET dyad can function as a single chromophore with the excitation wavelength corresponding to the donor excitation, and the emission wavelength characteristic for the acceptor emission. Thus, suitably chosen donor/acceptor pairs allow, in principle, for the independent tuning of the absorption and emission wavelengths. ET arrays have been utilized to increase the Stokes shift of fluorophores,[27−29] development of families of fluorophores with a common excitation wavelength and different emission wavelengths,[10,29−32] or a common emission wavelength and different excitation wavelengths[29] and have been applied for intracellular[27,30,31] and in vivo[10,30,31,33] imaging.

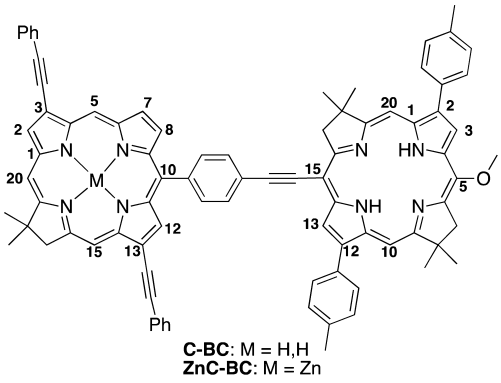

Figure 1. Phenylethynyl-linked chlorin−bacteriochlorin dyads studied by Holten, Lindsey, and co-workers.[29,33,38,39]

Applications of ET dyads for in vivo imaging necessitate both absorption of donor and emission of acceptor to fall within the 650−900 nm spectral window. Chromophores that have been used so far in ET dyads as donors and acceptors usually emit and/or absorb in the visible region,[25,26] while those manifesting both an excitation of donor and emission of acceptor in deep-red/near-IR regions have been much less explored.[10,29,33,34]

The idea to use hydroporpyrins as deep-red and near-IR absorbing donors and emitting acceptors in ET arrays originates from very intensive research on tetrapyrrolic ET arrays, which has aimed to understand and mimic the photosynthetic solar energy-converting systems in plants and bacteria.[35] While porphyrin−porphyrin and chlorin−chlorin ET arrays have been studied in great detail for more than three decades, the chlorin−bacteriochlorin ET dyads are known much less, and the systematic investigation of their photochemical properties has begun only recently. Tamiaki[36] and Mironov[37] reported an efficient energy transfer in chlorin−bacteriochlorin dyads, connected by flexible linkers. Holten, Lindsey, and co-workers performed detailed studies on chlorin−bacteriochlorin dyads, where macrocycles are linked by a phenylethynyl group at 10- and 15 (meso)-positions (Figure 1).[29,33,38,39] In the latter case, fast (4.8 ps^{-1}) and nearly quantitative ET (with quantum efficiency >0.99) has been determined, which results in exclusive emission from the bacteriochlorin (acceptor) moiety, even when the chlorin component was selectively excited.[29,38] The same authors demonstrated that chlorin−bacteriochlorin arrays show an excellent selectivity in excitation, due to the narrow absorption band of the chlorin donor.[29,33] Thus, in pairs of two chlorin−bacteriochlorin dyads (**C-BC** and **ZnC-BC**) with a common bacteriochlorin acceptor and different chlorin donors with an absorption maximum at 650 and 675 nm, respectively, each dyad can be excited with more than 90% selectivity, in the presence of the other one. Such high selectivity has been observed in a phantom tissue model[29] as well as in vivo in whole animal imaging.[33]

To further expand the potential of chlorin−bacteriochlorin dyads as fluorophores for multicolor in vivo imaging, we prepared a family of chlorin−bacteriochlorin dyads, possessing a common chlorin donor and bacteriochlorin acceptors equipped with a different set of auxochromes. Subsequently, we evaluated the spectral and photochemical properties of this type of architecture, specifically the brightness of acceptor fluorescence upon donor excitation. This set of dyads, excitable simultaneously at a common wavelength in the red region and emitting at different wavelengths in the near-IR region would provide a benchmark for evaluation of suitability of their optical properties for in vivo multicolor imaging.

dx.doi.org/10.1021/jo4016858 | J. Org. Chem. 2013, 78, 10678−10691

RESULTS AND DISCUSSION

1. Design. Several issues need to be considered when designing ET dyads which will exhibit bright fluorescence of the acceptor upon donor excitation. The first consideration is the efficiency of energy transfer between donor and acceptor. The excitation energy between tetrapyrrolic macrocycles can be transferred either through-space (via the Förster dipole−dipole interaction mechanism) or through-bond (when there is an appreciable donor−acceptor electronic communication).[38] It has been shown that in chlorin−chlorin and chlorin−bacteriochlorin dyads the dominant mechanism is through-space Förster energy transfer, even when a linker allows an electronic communication between donor and acceptor.[38,40]

The rate of the through-space Förster energy transfer is given by eq 1.[41]

$$k_{ET} = \frac{9000 \ln 10\kappa^2}{128\pi^5 n^4 N r^6 \tau_f} J \quad (1)$$

where κ is the orientation factor, τ_f is the fluorescence lifetime of donor in the absence of acceptor, r is the distance between donor and acceptor, n is the refractive index, N is Avogadro's constant, and J is the overlap integral, i.e., integral of the normalized donor fluorescence and acceptor extinction coefficient.

Thus, an efficient through-space energy transfer requires large spectral overlap, i.e., overlap between donor emission and acceptor absorption. This requirement restricts the choice of donor and acceptor pairs to the one possessing relatively small separation between their absorption bands. The second important issue which needs to be taken into account is the competitive electron transfer from or to the photoexcited dyad component. Hydroporphyrins in their excited states are potent electron donors, and the photoinduced electron transfer in dyads comprising hydroporphyrins produces a nonfluorescent ion pair.[39,40,42] The photoinduced electron transfer is specifically efficient in polar solvents, where the resulting ion pair is stabilized.[39,40,42] Consequently, extensive quenching of fluorescence intensity of chlorin−bacteriochlorin dyads in polar solvents (e.g., DMSO) has been observed.[39] Applications of chlorin−bacteriochlorin dyads in medicinal diagnosis would require their strong fluorescence in polar (aqueous) solvent. Therefore, the photoinduced electron transfer between dyad components must be inhibited, to achieve high fluorescence quantum yield from the dyad.

On the basis of the above consideration and keeping in mind the prior results obtained for chlorin−bacteriochlorin dyads,[38,39] we proposed the series of arrays shown in Chart 1. The key design features of proposed dyads are as follows: (1) chlorin and bacteriochlorin are connected through their respective 13 (β)-positions, along the axis, nearly colinear with the long-wavelength Q_y transition moments of both macrocycles; (2) a part of the chlorin−bacteriochlorin linker is also an auxochrome which tunes the spectral properties of bacteriochlorin; (3) an amide functionality is used to link the chlorin and bacteriochlorin. Because the terminal groups of the chlorin−bacteriochlorin linker function as auxochromes for chlorin and bacteriochlorin, the number of substituents to be installed on the both macrocycles is reduced; hence, the synthesis will be simplified. The amide group for linking was chosen for numerous reasons. First, the amide group reduces the electronic conjugation within the linker, which allows a variety of auxochromes at the 13-positions of both chlorin and bacteriochlorin moieties to be chosen, without providing strong electronic conjugation between both macrocycles. We also expect that the use of an amide linker, instead of the more conjugated one (e.g., phenyethynyl), would reduce electronic communication between both macrocycles and, in turn, accentuate the possible photoinduced electron/hole transfer between chlorin and bacteriochlorin. For example, the phenylethynyl linker assures efficient photoinduced electron transfer between donor and acceptor.[43] Finally, the use of an amide bond should facilitate the modular synthesis of dyads, as it allows a coupling of separately prepared chlorin and bacteriochlorin building blocks, under mild conditions, using well-established chemistry. Additionally, each dyad is also equipped with a 4-(methoxycarbonyl)phenyl substituent, placed at the 10-position of the chlorin component. This carboxylate moiety functions as a bioconjugatable group (upon conversion to active *N*-succinimide ester) for dyad attachment to biomolecules, which will serve as a targeting unit.

As a common donor, we utilized the 13-(4-aminophenyl)-chlorin derivative. As acceptors, we used a series of bacteriochlorins with different sets of substituents at the 3- and 13-positions, which function as auxochromes to tune the positions of absorption and emission bands of the given bacteriochlorin. The auxochrome at the 13-position of bacteriochlorin is a part of the chlorin−bacteriochlorin linker. One set of dyads (compounds **C-BC1** and **C-BC2**) contains a *N*-phenylbenzamide linker, whereas a second set (compounds **C-BC3**, **C-BC4**, and **C-BC5**) has a *N*-phenyl-4-ethynylbenza-

Chart 1. Structures of the Chlorin−Bacteriochlorin Dyads

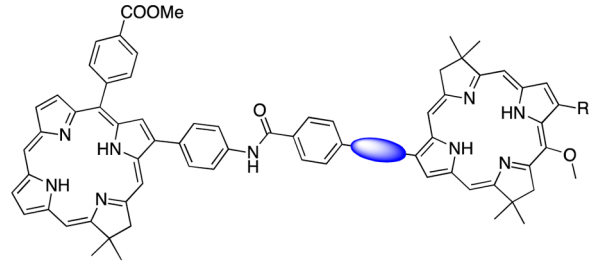

Dyad		R
C-BC1	None	H
C-BC2	None	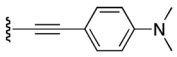
C-BC3	≡	
C-BC4	≡	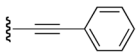
C-BC5	≡	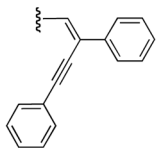

dx.doi.org/10.1021/jo4016858 | J. Org. Chem. 2013, 78, 10678−10691

mide linker. Consequently, the donor−acceptor distance in the second set of dyads is slightly longer than in the first set. The auxochromes installed at the 13-position of bacteriochlorin include none (hydrogen, in **C-BC1**), 4-(dimethylamino)-phenylethynyl (**C-BC2**), vinyl (**C-BC3**), phenylethynyl (**C-BC4**), and 2,4-diphenylbuta-1-en-3-ynyl (**CBC5**). The placement of different sets of auxochromes on the bacteriochlorin not only affects their spectral properties but should also alter the redox potential of the bacteriochlorin acceptor,[20] which, assuming the redox potential of the donor remains the same, should affect the rate of the putative electron transfer between dyad components. Taken together, examination of dyads **C-BC1−5** should allow the selection of sets of dyads with common excitation and distinctive emission wavelengths and, additionally, allows the evaluation of the influence of the donor−acceptor linker length and acceptor redox potential on the energy and electron transfer properties of chlorin−bacteriochlorin dyads. Chart 2 presents the structures of chlorin and bacteriochlorin benchmarks for donor (**C-NHPh**) and acceptors (**BC1−5**).

2. Syntheses. The chlorin component, 13-(4-aminophenyl)chlorin **C-NH$_2$**, of the dyads has been prepared following the reported procedure for a synthesis of 13-substituted chlorins (Scheme 1).[24,44] Thus, the required 1,2-dibromo-9-formyldipyrromethane **3** was obtained by Vilsmeier formylation and subsequent dibromination[44] of 5-(4-(methoxycarbonyl)phenyl)dipyrromethane **1**.[45] The resulting **3** was semipurified with column chromatography and immediately used in the next step. 13-Bromochlorin **C-Br** has been obtained by condensation of **3** and previously reported tetrahydrodipyrrin **4**[46] in three steps (Scheme 1):[24,44] acid-catalyzed condensation, oxidative cyclization, and TFA-induced demetalation of the resulting zinc chlorin. The overall yield of chlorin synthesis from **2** is 10%. The 4-aminophenyl group was installed via Suzuki coupling, utilizing modified published conditions,[19] in 77% yield. The benchmark monomer, N-benzoylated **C-NHPh**, has been prepared by EDC-mediated coupling of **C-NH$_2$** with benzoic acid, in DMF, in the presence of DMAP, in 87% yield (Scheme 1).

Bacteriochlorin Components. Bacteriochlorin components of the dyads are derivatives of 5-methoxybacteriochlorin, each having different substituents at the 3- and 13-positions. Substituents at the 13-position, in each case, are also equipped with a carboxyl group, which subsequently functions as a synthetic handle to attach the desired bacteriochlorin to the chlorin **C-NH$_2$**. The ester derivatives of bacteriochlorin components **BC1−5**, which are precursors for dyads, also serve as benchmark acceptors (Chart 2). For synthesis of bacteriochlorins **BC1−5**, we utilized a recently developed method of selective functionalization of 3,13-dibromo-5-methoxybacteriochlorins **BC-Br$_2$**.[47] This method takes advantage of the diminished reactivity of bromine at the 3-position toward palladium-catalyzed cross-coupling, presumably due to the steric effect of the adjacent methoxy group. Bacteriochlorins **BC3−5** have been prepared previously via this method.[47] For synthesis of **BC1,2**, we extended the selective functionalization of **BC-Br$_2$**, which was previously demonstrated for the Sonogashira reaction only, on the Suzuki cross-coupling. Thus, Suzuki reaction of **BC-Br$_2$**[48] with (4-(methoxycarbonyl)-phenyl)pinacolborane provided 13-(methoxycarbonylphenyl)-3-bromobacteriochlorin **BC-BrCOOMe** in 74% yield (Scheme 2). The **BC-BrCOOMe** was then further derivatized at the 3-position. Palladium-catalyzed reduction of **BC-BrCOOMe**, using a modified published procedure,[17] provides the 3-desbromo **BC1** in 93% yield. Sonogashira reaction of **BC-BrCOOMe** with 4-ethynyl-*N*,*N*-dimethylaniline provides **BC2** in 77% yield (Scheme 2).

The synthesis of (*Z*)-2,4-diphenylbut-2-en-3-yne-substituted bacteriochlorin **BC5** was described previously;[47] however, its structure was only tentatively assigned based on the NMR and MS data. Here, we ultimately confirmed the structure of **BC5** by X-ray crystallography.[49] The X-ray structure (see Figure S5, Supporting Information) confirms the presence of the 2,4-diphenylbuta-1-en-3-ynyl substituent at the 3-position of bacteriochlorin, with *Z* configuration of the carbon−carbon double bond (see Supporting Information for more detailed discussion of the **BC5** structure).

Chart 2. Structures of Benchmark Donor and Acceptors

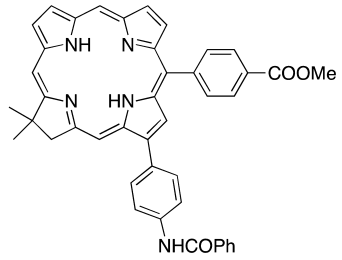

C-NHPh

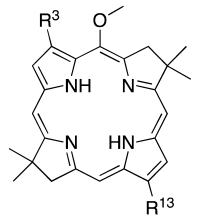

Compound	R^3	R^{13}
BC1	H	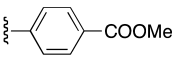
BC2	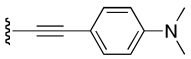	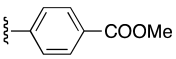
BC3		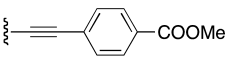
BC4	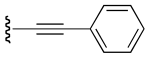	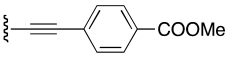
BC5	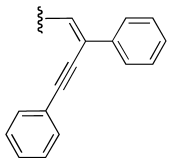	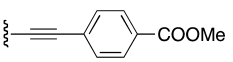

dx.doi.org/10.1021/jo4016858 | J. Org. Chem. 2013, 78, 10678−10691

Scheme 1

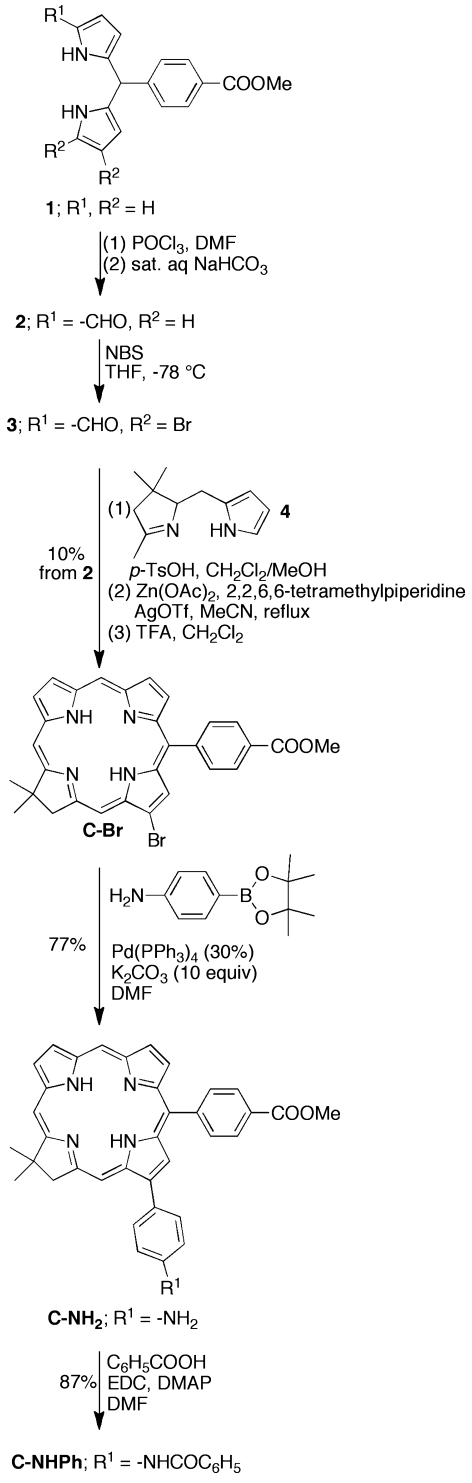

Scheme 2

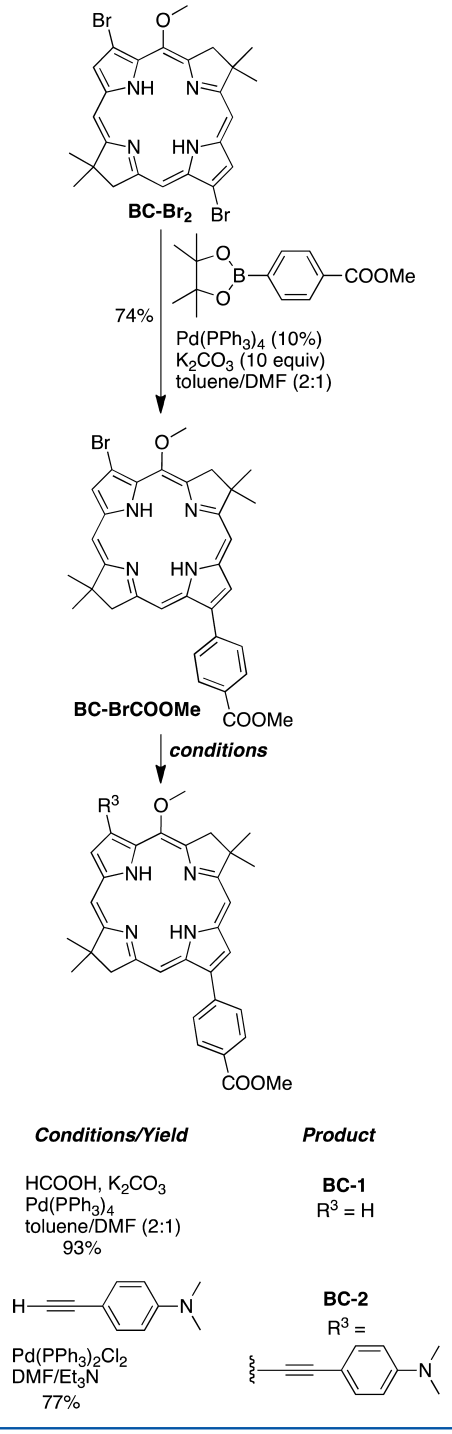

The final dyads were assembled by the reactions of carboxylic acids, obtained by basic hydrolysis of **BC1**−**5**, with the amine function of **C-NH$_2$** (Scheme 3). The amide formation, mediated by EDC, in the presence of DMAP, provides the final dyads in 40−73% yields.

The ester groups in selected dyads (**C-BC1**, **C-BC2**, and **C-BC5**) were hydrolyzed (using aqueous NaOH in MeOH/THF) and reacted with *N*-hydroxysuccinimide (NHS) in the presence of EDC and DMAP, to provide bioconjugatable *N*-succinimide esters in 74%, 56%, and 43% yields, respectively (Scheme 3).

3. Characterization. The final dyads as well as benchmark monomers and intermediates were fully characterized using ^{1}H and ^{13}C NMR, LD-MS, and high resolution MS (we were not able to collect a good-quality ^{13}C NMR spectra for **C-BC4** and **C-BC5** because of solubility issues). The spectroscopic data are consistent with the proposed structures. The ^{1}H NMR spectra for each dyad contain proton signals from both chlorin and bacteriochlorin, with chemical shifts comparable to those for corresponding benchmark monomers (see Supporting Information for examples).

dx.doi.org/10.1021/jo4016858 | J. Org. Chem. 2013, 78, 10678−10691

Scheme 3

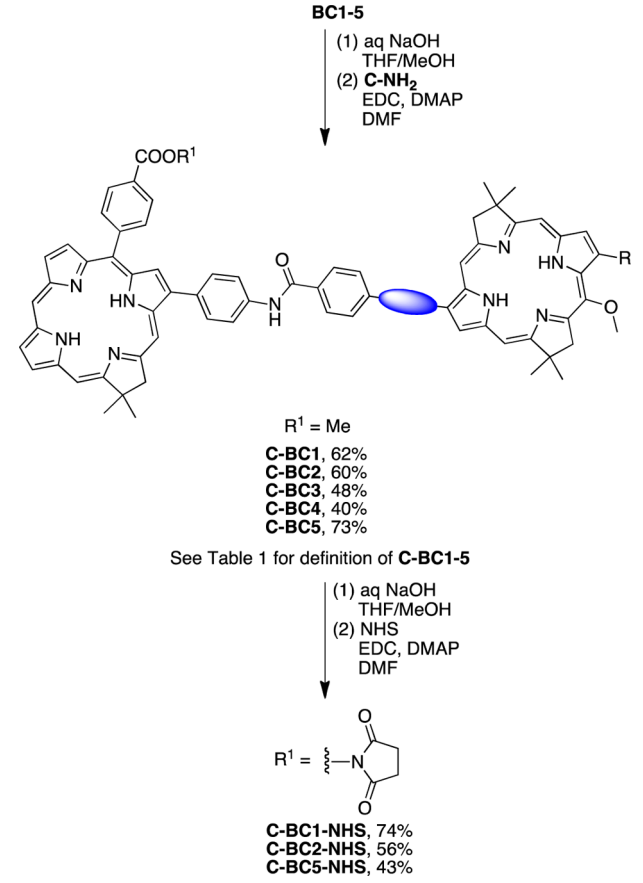

4. Optical Properties. *Absorption.* Both absorption and emission properties of dyads and benchmark monomers were determined in toluene and DMF. Absorption spectra of benchmark donor **C-NHPh** and acceptors **BC1**−**5** are presented in Figure 2, and their maxima are listed in Table 1. The absorption spectrum of **C-NHPh** matches that of the analogous 13-phenylchlorin reported previously[16] and shows an intensive Q_y band at λ = 646 nm. The extinction coefficients for the Q_y band of **C-NHPh** are 3.63 × 10^4 M^{-1}·cm^{-1} and 3.96 × 10^4 M^{-1}·cm^{-1} in toluene and DMF, respectively.

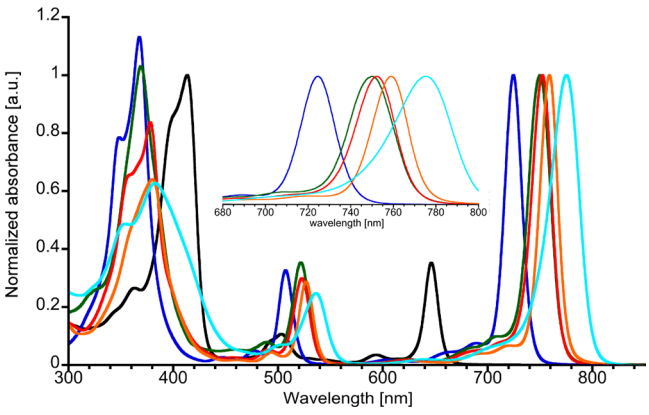

Figure 2. Absorption spectra of benchmarks chlorin **C-NHPh** (black) and bacteriochlorins **BC1** (blue), **BC2** (green), **BC3** (red), **BC4** (orange), and **BC5** (light-blue). Spectra of bacteriochlorins are normalized at their Q_y bands. All spectra were measured in toluene and are normalized at the maxima of Q_y bands of bacteriochlorins and the B band of chlorin.

Absorption spectra of bacteriochlorin benchmark acceptors (Figure 2 and Table 1 spectra of **BC3**, **BC4**, and **BC5** have been reported previously[47]) show intensive Q_y bands at wavelengths above 700 nm, a Q_x band at 520−535 nm, and a broad band at ∼375 nm, consisting of B_x and B_y bands. As expected, the Q_y bands exhibit a gradual bathochromic shift with increasing conjugation of auxochromes at the 3- and 13-position.[15,17] Thus, 3-unsubstituted-13-phenylbacteriochlorin **BC1** exhibits a Q_y band at 725 nm, 3-(4-(dimethylamino)-phenylethynyl)-13-phenylbacteriochlorin **BC2** at 750 nm, 3-vinyl-13-phenylacetylenebacteriochlorin **BC3** at 752 nm, 3,13-diphenylethynylbacteriochlorin **BC4** at 759 nm, and 3-(2,4-diphenylbut-1-en-3-ynyl)-13-phenylethynylbacteriochlorin **BC5** at 775 nm. The Q_y bands for most of the derivatives are narrow with the fwhm in the range 19−25 nm, with the exception of **BC5** for which the Q_y band is substantially broader (34 nm). The broadening of the absorption band for **BC5** might arise from the conformational heterogeneity of the complex substituent at the 3-position. It is expected that the twisting along single carbon−carbon bonds in the buta-1-en-3-yne substituent reduces the degree of electronic conjugation and in turn leads to the slight hypsochromic shift of the Q_y band, which overall causes the observed broadening in **BC5**.

For each benchmark monomer, the position and shape of the absorption bands are nearly independent of the solvent polarity and are essentially the same in toluene and in DMF (Table 1). Changing the solvent from toluene to DMF results in a slight hypsochromic shift (1 nm) of the absorption maxima of each band and slight broadening of the Q_y band.

Absorption spectra of dyads in toluene (Figure 3, Table 1) are essentially the sum of the spectra of their benchmark components, which indicates that only weak ground-state interactions occur between dyad components. Thus, the spectrum of each dyad contains absorption peaks characteristic for the chlorin donor: Q_y band at 646 nm, and B bands with a maximum at 413 nm. Each spectrum also contains the Q_y band of the bacteriochlorin, with the maximum centered at the same wavelength as its corresponding benchmark monomer. The ratio of absorbance of Q_y bands of chlorin to bacteriochlorin varied from 0.33 for **C-BC4** to 0.59 for **C-BC5**. This reflects the difference in extinction coefficients for Q_y bands of chlorins and bacteriochlorins. The reported values of extinction coefficients for similar synthetic bacteriochlorins are in the range of 110 000−130 000 M^{-1}·cm^{-1}.[50] Similar to the monomers, shapes and positions of absorption maxima for dyads vary only slightly with solvent polarity (Table 1).

Emission Properties. Emission spectra of benchmark chlorin and bacteriochlorin monomers (Figure 4, Table 2) are similar to those for reported previously analogous chlorins and bacteriochlorins.[15,17,19] Thus, benchmark chlorin **C-NHPh** exhibits in toluene a strong emission $Q_y(0,0)$ band at 650 nm. Benchmark bacteriochlorins exhibit, in toluene, strong $Q_y(0,0)$ bands with the Stokes shift in the range of 7−13 nm. The fwhm of emission bands for bacteriochlorins are in the range of 21−28 nm, with the exception of **BC5**, for which fwhm is 35 nm. The markedly broader emission band for **BC5** is presumably due to the conformational heterogenity within the enyne substituent. The positions of emission maxima only slightly depend on the solvent polarity and follow the same trend as was observed for Q_y absorption bands. The quantum yields of fluorescence for benchmark bacteriochlorin monomers

dx.doi.org/10.1021/jo4016858 | J. Org. Chem. 2013, 78, 10678−10691

Table 1. Absorption Properties of Chlorin−Bacteriochlorin Dyads and Corresponding Benchmark Monomers

compd	Q_{yBC}[a] (toluene)	Q_{yBC}[a] (DMF)	Q_{xBC}[b] (toluene)	Q_{xBC}[b] (DMF)	B[c] (toluene)	B[c] (DMF)	Q_C/Q_{BC}[d] (toluene)	Q_C/Q_{BC}[d] (DMF)	fwhm Q_{yBC}[e] (toluene)	fwhm Q_{yBC}[e] (DMF)
C-BC1	725	724	507	505	368, 413	366, 412	0.47	0.47	19	20
C-BC2	750	749	521	518	370, 384, 413	368, 393, 412	0.45	0.47	25	29
C-BC3	752	751	523	521	380, 413	379, 412	0.43	0.42	22	23
C-BC4	759	758	527	525	391, 413	394, 412	0.33	0.32	20	21
C-BC5	776	775	535	533	413	412	0.59	0.59	34	36
BC1	725	724	507	506	368	366	–	–	19	20
BC2	750	749	522	520	369	368	–	–	25	28
BC3	752	752	523	522	378	376	–	–	22	23
BC4	759	758	527	525	380	379	–	–	20	21
BC5	775	776	536	536	382	383	–	–	33	34
C-NHPh	646	645	503	503	413	412	–	–	15	17

[a]The wavelength of the maximum of the bacteriochlorin Q_y band in toluene and DMF, respectively [nm]. [b]The wavelength of the maximum of the bacteriochlorin Q_x band in toluene and DMF, respectively [nm]. [c]The wavelengths of the maxima of the bacteriochlorin and/or chlorin B bands in toluene and DMF, respectively. [d]Ratio of absorbance at the maxima of Q_y bands of chlorin and bacteriochlorin components in dyads, in toluene and DMF, respectively [nm]. [e]Full-width-at-half-maximum for Q_y band of bacteriochlorin in toluene and DMF, respectively [nm].

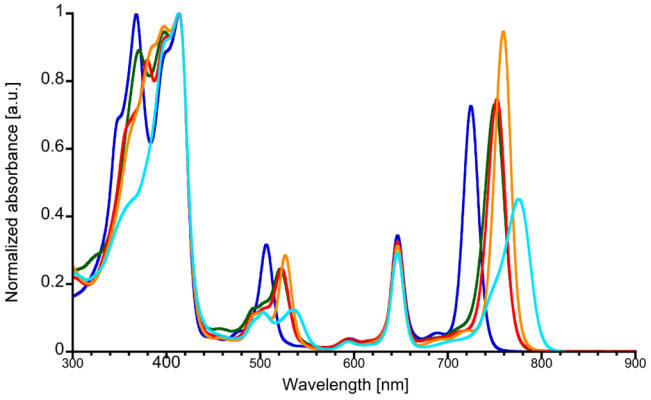

Figure 3. Absorption spectra of dyads: **C-BC1** (blue), **C-BC2** (green), **C-BC3** (red), **C-BC4** (orange), and **C-BC5** (light-blue). All spectra are normalized at the maximum of the B band of the chlorin component (413 nm). All spectra were measured in toluene.

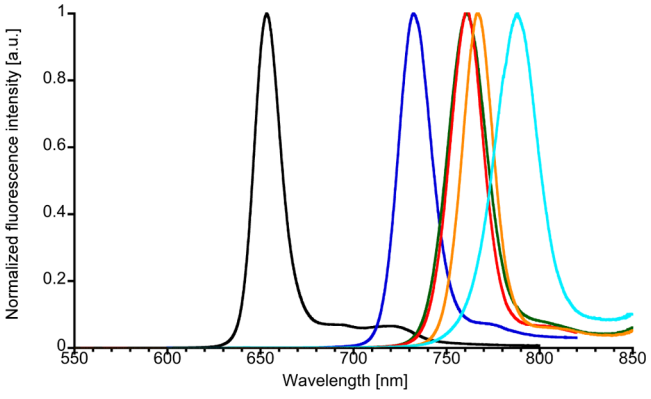

Figure 4. Normalized emission spectra of benchmarks chlorin **C-NHPh** (black) and bacteriochlorins **BC1** (blue), **BC2** (green), **BC3** (red), **BC4** (orange), and **BC5** (light-blue). All spectra were measured in toluene. Chlorin was excited at the maximum of its B band (413 nm), while bacteriochlorins were excited at the corresponding maxima of their Q_x bands.

in toluene and DMF are given in Table 2 and are in the range 0.17−0.25, which is consistent with data reported previously for similar synthetic bacteriochlorins.[15] Fluorescence of bacteriochlorin monomers is moderately quenched in DMF, where quantum yields are 0.84−0.90 fold of those determined in toluene. It is worth noting that the fluorescence quantum yield for **BC2**, substituted with an electron-rich 4-(dimethylamino)-phenylethynyl substituent, is relatively high in both toluene (0.25) and in DMF (0.21), which indicates that putative electron transfer from the electron-rich *N*,*N*-dimethylphenyl moiety to bacteriochlorin is negligible. Fluorescence quantum yield for the benchmark chlorin monomer **C-NHPh** in toluene is 0.27 and is only slightly quenched in DMF (0.26).

Emission spectra of each dyad in toluene (Figure 5) predominantly consist of the emission band of the corresponding bacteriochlorin component, whereas emission of the chlorin is significantly quenched, regardless of excitation wavelength. Bacteriochlorin emission is predominant even when the dyad is

Table 2. Emission Properties of Chlorin−Bacteriochlorin Dyads and Benchmark Monomers[a]

dyad	λ_{max} (toluene)	λ_{max} (DMF)	fwhm (toluene)	fwhm (DMF)	Φ_f[b] (toluene)	Φ_f[b] (DMF)
C-BC1	732	732	21	22	–	–
C-BC2	761	762	26	28	–	–
C-BC3	761	760	22	22	–	–
C-BC4	767	766	20	21	–	–
C-BC5-NHS[c]	788	788	28	29	–	–
BC1	732	732	21	22	0.22	0.20
BC2	761	762	25	28	0.25	0.21
BC3	761	760	21	22	0.22	0.19
BC4	767	766	20	21	0.23	0.21
BC5	788	788	28	29	0.20	0.17
C-NHPh[d]	653	652	17	18	0.27	0.26

[a]All samples containing a bacteriochlorin were excited at the maximum of Q_x band of the bacteriochlorin component. [b]Fluorescence quantum yield of benchmark donor and acceptors. Fluorescence quantum yields were determined in nondegassed solvents, using tetraphenylporphyrin in nondegassed toluene (Φ_f = 0.07[15]) as a standard and were corrected for solvent refractive index. The estimated experimental error is ±5%. [c]Data listed were determined for the corresponding NHS-ester, due to the presence of trace amount of nonseparable, red-fluorescent contamination in the sample of **C-BC5**. [d]Excited at the maximum of the B band.

dx.doi.org/10.1021/jo4016858 | J. Org. Chem. 2013, 78, 10678−10691

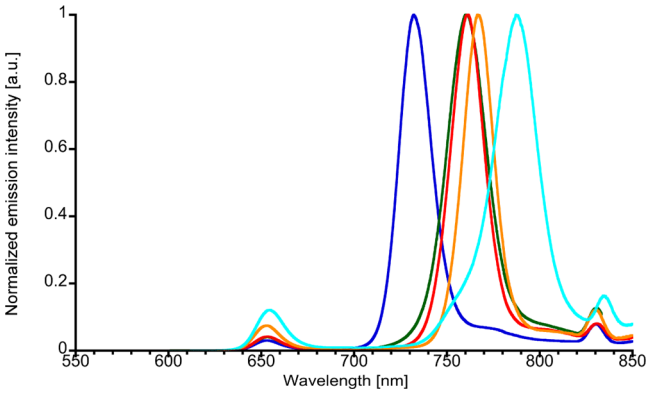

Figure 5. Normalized emission spectra (in toluene) of dyads: **C-BC1** (blue), **C-BC2** (green), **C-BC3** (red), **C-BC4** (orange), and **C-BC5-NHS** (light-blue). All dyads were excited at the maximum of B band of the chlorin component (413 nm for **C-BC1−4**, 414 nm for **C-BC5-NHS**). The humps at ∼825−830 nm are due to the subharmonic scattering from the excitation beam.

excited at the maximum of the chlorin component absorption (413 nm), where bacteriochlorin shows a negligible absorption. The wavelengths of bacteriochlorin emission for dyads are identical to those for the corresponding benchmark monomers. The fluorescence excitation spectra of dyads (not shown), monitored at wavelengths where bacteriochlorin components of dyads emit almost exclusively, closely match the corresponding absorption spectra. These observations are consistent with an efficient energy transfer from chlorin to bacteriochlorin. Fluorescent quantum yields of the bacteriochlorin component in dyads, when chlorin is selectively excited, in toluene and DMF (Φ_{donor} Table 3) are lower than for corresponding benchmark monomers. The Φ_{donor} values are in the range of 0.155−0.23 in toluene, whereas in DMF are in the range of 0.12−0.185. In toluene the fluorescence of the acceptor in dyads, when the donor is excited, is moderately quenched for **C-BC5** and **C-CB2** (0.78 and 0.92-fold, compared to the corresponding monomers), while for other dyads is fairly comparable with the respective monomers. At the same time, Φ_{donor} in DMF is markedly lower than Φ_f for corresponding monomers in each dyad, ranging from 0.69-fold for **C-BC2** to 0.88-fold for **C-BC4**, of their corresponding benchmark bacteriochlorins.

Estimation of the Efficiency of Energy Transfer and Fluorescence Quenching in Chlorin−Bacteriochlorin Dyads. The application of chlorin−bacteriochlorin dyads for biological and biomedical imaging would require their bright fluorescence in media of different polarity, including aqueous solution. Because fluorescence quantum yields of bacteriochlorin components in dyads (when donor is excited) are markedly lower than for corresponding benchmark monomers, it would be instructive to evaluate factors which affect the fluorescence quantum yield of bacteriochlorin components in dyads, in both nonpolar and polar solvents. The fluorescence quantum yields of bacteriochlorin acceptors in dyads, when the chlorin donor is selectively excited, depend on (a) intrinsic fluorescence quantum yields of the bacteriochlorin component, (b) efficiency of energy transfer from chlorin to bacteriochlorin, and (c) efficiency of quenching processes, e.g., electron/hole transfer from photoexcited dyad components. The intrinsic fluorescence quantum yields of the bacteriochlorin acceptor are identical with the quantum yields of bacteriochlorin benchmarks and are given in Table 2.

The efficiency of energy transfer (ETE) from chlorin to bacteriochlorin was estimated using steady-state emission spectroscopy, by comparison of the fluorescence quantum yields of acceptor (bateriochlorin) when directly excited with those obtained when the donor (chlorin) component was selectively excited.[27c]

$$\mathrm{ETE} = \frac{\Phi_{donor}}{\Phi_{accep}} \qquad (2)$$

where Φ_{donor} is the fluorescence quantum yield of bacteriochlorin acceptor, when the chlorin donor is selectively excited; Φ_{accep} is the fluorescence quantum yield of the same bacteriochlorin, when directly excited.

ETE defined in such a way (which is different than ET quantum efficiency ϕ_{ET}, commonly used for characterization of ET dyads;[38,40] see discussion in Supporting Information) directly shows how much fluorescence intensity is lost when energy is transferred, due to both "leakage" of fluorescence intensity by donor emission and putative quenching processes, which are competitive with energy transfer (e.g., electron/hole transfer from photoexcited donor).

For direct excitation of bacteriochlorin component in dyads, we have chosen the maximum of the Q_x band of the bacteriochlorin (∼510−525 nm), where bacteriochlorins absorb predominantly and the chlorin component shows little absorbance. The chlorin component was selectively excited at the maximum of its B band (412−414 nm), where bacteriochlorins show a negligible absorbance. The results are given in Table 3. Energy transfer efficiency in toluene is generally high for dyads **C-BC1−4**, ranging from 0.91 to 0.98 and somehow lower for **C-BC5** (0.86). The ETE in DMF, ranging from 0.77 to 0.89 is markedly lower for each dyad than those determined in toluene. The lower ETE in DMF is also manifested by a noticeably higher intensity of chlorin component emission in DMF. Nevertheless, ETEs in both

Table 3. Photochemical Data for Chlorin−Bacteriochlorin Dyads

dyad	Φ_{donor}[a] (toluene)	Φ_{accep}[b] (toluene)	Φ_{donor}[a] (DMF)	Φ_{accep}[b] (DMF)	ETE[c] (toluene)	ETE[c] (DMF)	ϕ_q[d] (toluene)	ϕ_q[d] (DMF)
C-BC1	0.225	0.23	0.16	0.18	0.98	0.89	1.05	0.94
C-BC2	0.23	0.245	0.145	0.195	0.94	0.75	0.98	0.93
C-BC3	0.21	0.23	0.17	0.195	0.91	0.89	1.05	1.03
C-BC4	0.22	0.23	0.185	0.21	0.96	0.88	1.00	1.0
C-BC5[e]	0.155	0.18	0.12	0.155	0.86	0.77	0.91	0.91

[a]Fluorescence quantum yields of bacteriochlorin dyad components excited at the maximum of the B band of the chlorin component. [b]Fluorescence quantum yields of bacteriochlorin dyad components excited at the maximum of the Q_x band of bacteriochlorin. [c]Energy transfer efficiency calculated from eq 2. [d]The ratio of fluorescence quantum yield of bacteriochlorin component in dyads (when excited at the maximum of the bacteriochlorin Q_x band) to the fluorescence quantum yield of the corresponding bacteriochlorin benchmark monomer.

dx.doi.org/10.1021/jo4016858 | J. Org. Chem. 2013, 78, 10678−10691

solvents are relatively high, given the separation between the maxima of donor emission and acceptor absorbance, ranging from 72 nm for **C-BC1** to 122 nm for **C-BC5**. Apparently, there is a sufficient spectral overlap between donor emission and acceptor absorption, mainly due to the overlap of the $Q_y(1,0)$ emission band of chlorin with the vibronic absorption band of bacteriochlorins (see Figure S3, Supporting Information). We cannot exclude also a contribution of the through-bond energy transfer mechanism. The origin of reduced ETE in DMF is not obvious. The less efficient energy transfer in polar solvents (toluene vs benzonitrile) has been reported previously for amide-linked porphyrin–porphyrin dyads,[51] as well as diphenylethynyl-linked chlorin–chlorin dyads[40] (in all these cases quantum efficiency of ET was determined; see discussion in Supporting Information). The comparison of refractive indexes for both solvents (n_{tol} = 1.496, n_{DMF} = 1.4305) suggests that energy transfer should be more efficient in DMF than in toluene (because $k_{ET} \sim 1/n^4$; see eq 1). The similarity of absorption and emission spectra of both donor and each acceptor in toluene and DMF suggested that only slight differences in spectral overlap would be expected; thus, this factor should not account for the observed differences in ETE in both solvents. The possible reasons would include a combination of (a) slight changes in fluorescence quantum yield and lifetime of the donor in both solvents, (b) solvent-induced conformational changes in the linker, leading to increasing chlorin–bacteriochlorin distance and/or changes in their mutual orientation, and (c) competitive electron/hole transfer from photoexcited chlorin to bacteriochlorin. More detailed, time-resolved spectroscopic examination is required to delineate the contribution of these factors.

The electron/hole transfer from photoexcited dyad component is potentially highly detrimental for dyad fluorescence brightness. Chlorins and bacteriochlorins are known as efficient electron donors in their excited states and might also function as electron acceptors, and if it is the case, electron transfer between tetrapyrrolic macrocycles leads to formation of the nonfluorescent charge-separated state.[39,40,42] The electron transfer is accentuated in polar solvents, which stabilizes the resulting charge-separated ion radical pair. We estimated the extent of quenching of the acceptor fluorescence in dyads in nonpolar (toluene) and polar (DMF) solvents. For that, we compared the fluorescence quantum yields of the bacteriochlorin acceptor in dyads (determined when the acceptor is directly excited at its corresponding Q_x band maximum) and fluorescence quantum yields of the corresponding benchmark monomers in each solvent.

$$\phi_q = \frac{\Phi_{accep}}{\Phi_{benchmark}} \quad (3)$$

where Φ_{accep} is the florescence quantum yield of the bacteriochlorin acceptor in the dyad (when directly excited), and $\Phi_{benchmark}$ is the fluorescence quantum yield of the corresponding benchmark.

The resulting "quenching ratio" ϕ_q determined in toluene and DMF is given in Table 3. The data show that there is a little quenching of fluorescence in toluene for dyad **C-BC5**. In other cases the fluorescence quantum yield of acceptor in the dyad is equal to or slightly higher than that for benchmark monomers. In DMF some insignificant quenching for dyads **C-BC1**, **C-BC2**, and **C-BC5** was observed (Table 3), while no quenching was observed for **C-BC3** and **C-BC4**.

To further evaluate the potential of chlorin–bacteriochlorin dyads for biological imaging, we examined dyad **C-BC4** in an aqueous buffer/surfactant mixture. We used PBS (pH 7.4)/Triton X-100 (0.35% v/v) mixture. The absorption spectrum of **C-BC4** (see Supporting Information, Figure S4, concentration of dyad ~0.75 mM) closely resembles that in DMF and in toluene, indicating that there is no aggregation of the dyad. The Φ_{donor} was determined as 0.14, ETE was estimated as 0.75, and the quenching of fluorescence, ϕ_q compared to the benchmark in toluene was estimated as 0.79.

The results discussed above indicate that the ETE is reasonably high and quenching due to putative hole or electron transfer from photoexcited bacteriochlorin is rather insignificant in the amide-linked chlorin–bacteriochlorin dyads reported here. The major factor which accounts for diminished fluorescence quantum yields of acceptors in dyads in polar solvent is the reduced ETE from chlorin to bacteriochlorin.

Chlorin–Bacteriochlorin Dyads as Potential Fluorophores for Multicolor Imaging. Here we discuss the overlap of the emission bands of chlorin–bacteriochlorin dyads reported here, to evaluate their usefulness as fluorophores for multicolor imaging. For that, we looked at how selectively emission from the individual dyad can be detected in the presence of other dyads. Previously, Holten and co-workers performed a detailed comparison of selectivity of excitation and emission detection for phenylethynyl-linked chlorin–bacteriochlorin dyads and commercially available Alexa dyes with similar excitation/emission wavelengths.[29] Here, we analyze the selectivity for emission detection of bacteriochlorin acceptors in dyads. Inspection of Figure 5 clearly shows that dyads **C-BC2**, **C-BC3**, and **C-BC4** have strongly overlapping emission bands, with the maxima centered at 761–767 nm, whereas emission bands of **C-BC1** and **C-BC5** are well-separated from the other bands (with maxima at 732 and 788 nm, respectively). Thus, three dyads, with minimal emission overlap, can be selected: **C-BC1**, **C-BC5**, and one from the **C-BC2–4** series. We chose three dyads, **C-BC1**, **C-BC3**, and **C-BC5**, to estimate their spectral overlap; **C-BC3** was chosen because its emission maxima at 660 nm is equally separated from that of both **C-BC1** and **C-BC5** (28 nm) and its emission band is somehow narrower than that for **C-BC2**. Figure 6 presents the emission

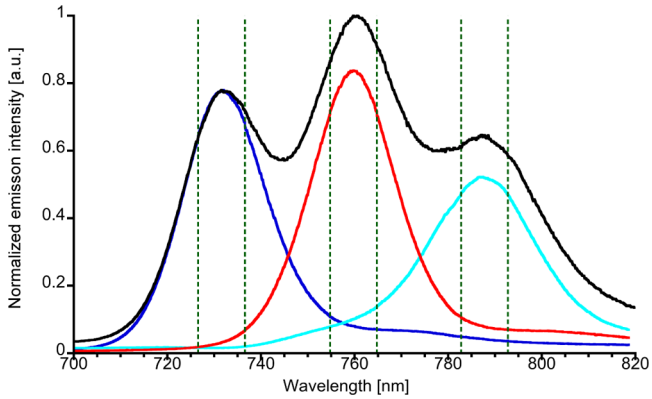

Figure 6. Absorption spectra of the mixture of **C-BC1**, **C-BC3**, and **C-BC5-NHS** (black) and spectra of each individual dyad: **C-BC1** (blue), **C-BC3** (red), and **C-BC5-NHS** (light blue). All spectra were measured in DMF, and each sample was excited at 645 nm. The concentration of each dyad (in the mixture and individually) was adjusted to an equal absorbance at 645 nm.

dx.doi.org/10.1021/jo4016858 | J. Org. Chem. 2013, 78, 10678–10691

spectra of the mixture **C-BC1**, **C-BC3**, and **C-BC5** in DMF, excited at 645 nm (black trace), together with the emission spectra of each individual component. The concentration of each dyad in the mixture was adjusted to achieve approximately equal absorbance at 645 nm. The spectrum of each component was recorded at an equal dyad absorbance at 645 nm, and then each spectrum was normalized so that the maximum intensity of **C-BC1** was the same as the maximum of the corresponding peak in the mixture. The vertical lines in Figure 6 represent 10-nm slices, centered at the maximum of each peak, which correspond to the 10-nm step size of the tunable emission filter, usually used for whole-animal, multicolor fluorescence imaging.[3−5] The spectrum clearly shows three well-resolved peaks, with maxima at 732, 760, and 788 nm, fully corresponding to the maximum of each dyad in the mixture. Thus, in such a mixture, more than 90% of the total fluorescence intensity, collected by the 10-nm wide detection channel, centered at 732 nm, would come from **C-BC1**. Similarly, 83% and 80% of total light intensity, collected in detection channels centered at 760 and 788 nm, would come from **C-BC3** and **C-BC5**, respectively. This selectivity should greatly facilitate the use of chlorin−bacteriochlorin dyads in multicolor fluorescence detection.

CONCLUSION AND OUTLOOK

We synthesized a family of chlorin−bacteriochlorin energy-transfer dyads with a common energy donor and different energy acceptors. The proposed molecular design allows for relatively straightforward incorporation of bacteriochlorins with different emission properties into dyads. The resulting dyads exhibit efficient energy transfer from chlorin to bacteriochlorin, even for large separation of chlorin emission and bacteriochlorin absorption maxima. Overall, the dyads reported here show a range of optical properties that makes them attractive candidates for application for in vivo multicolor imaging. These properties include a common excitation band in the red spectral window, narrow and tunable emission in the near-IR spectral window, and relatively bright fluorescence in solvents of different polarity. Their ultimate application for in vivo imaging requires addressing a number of issues concerning their toxicity, biocompatibility, intracellular delivery, photo- and chemostability, etc. The lack of cellular and organ toxicity is an important issue, when considering in vivo applications. The toxicity of dyads described here has not been tested yet; however, previous reports on application of hydroporphyrins for in vivo imaging[21−23] suggested that hydroporphyrins, in general, do not show toxicity that would prevent them from being used in vivo. Application of proposed dyads in biomedical imaging requires water solubility and methods for their delivery to the target cells or organs. The dyads reported here are hydrophobic and water-insoluble; however, this issue can be surmounted in a variety of ways, e.g., by attachment of large biomolecules (e.g., proteins or antibodies) which may function as both water-solubilizing moieties and targeting vehicles.[21] Alternatively, hydrophobic dyads may be encapsulated into hydrophilic nanostructures (e.g., polymersomes), as reported for other arrays of tetrapyrrolic macrocycles.[52] Finally, hydrophilic, water-soluble analogues of dyads **C-BC1−5** can be prepared and used, because both synthetic, water-soluble chlorins[53] and bacteriochlorins[54] have been reported.

On the other hand, time-resolved spectroscopy and electrochemical studies should provide further insight into the kinetics and mechanism of the energy transfer and the exact nature of the processes responsible for fluorescence quenching in dyads. This knowledge would be helpful in further optimization of the optical properties of dyads for specific imaging purposes. All these aspects are currently being addressed in our laboratory.

EXPERIMENTAL SECTION

General. ^{1}H NMR spectra (400 MHz) and ^{13}C NMR (100 MHz) spectra were collected at room temperature in $CDCl_3$ unless noted otherwise. Chemical shifts (δ) were calibrated using solvent peaks (^{1}H signals (residual proton signals): 7.26 ppm for chloroform; ^{13}C signals: 77.0 for $CDCl_3$; 25.4 ppm for THF-d_8). All solvents and commercialy available reagents were used as received. Commercially available anhydrous DMF and toluene were used without further purifications. All palladium coupling reactions and EDC-mediated amide syntheses were performed in comercially available anhydrous solvents (toluene and DMF). All palladium coupling reactions were performed under nitrogen using standard Schlenck glassware, and the reaction mixture was degassed each time using a freeze−thaw cycle (three times). All fluorescence spectra were collected in nondegassed, air-equilibrated solvents, with absorbance at the excitation wavelength (or bacteriochlorin Q_y band, whichever is higher) < 0.1. Fluorescence quantum yields were determined using tetraphenylporphyrin in nondegassed toluene as a standard (Φ_f = 0.07).[15] The FT-ICR analyzer was used for ESI HRMS. Known compounds: dipyrromethane **1**,[45] tetrahydrodipyrrin **4**,[46] bacteriochlorins **BC-Br$_2$**,[48] **BC3**,[47] **BC4**,[47] and **BC5**[47] were obtained following the reported procedures.

1-Formyl-5-(4-(methoxycarbonyl)phenyl)dipyrromethane (2). Vilsmeier reagent was prepared following a reported procedure.[44] A sample of DMF (10 mL) was treated with $POCl_3$ (2.40 mL, 25.8 mmol) under nitrogen and stirred for 10 min at 0 °C. The resulting mixture was added to a solution of 5-(4-(methoxycarbonyl)phenyl)-dipyrromethane **1**[45] (6.24 g, 22.3 mmol) in DMF (40 mL) at 0 °C. After 1.5 h, saturated $NaHCO_3$ solution (100 mL) was added. The resulting mixture was stirred overnight and extracted with ethyl acetate. Organic layers were combined, washed (brine), dried (Na_2SO_4), and concentrated. Column chromatography [hexane/ethyl acetate (1:1)] provided unreacted starting material (0.864 g) and desired product (white powder, 3.86 g, 65%): mp 140−141 °C; ^{1}H NMR ($CDCl_3$, 400 Hz), 9.85 (br, 1H), 9.25 (s, 1H), 8.38 (br, 1H), 7.95 (d, J = 8.2 Hz, 2H), 7.22 (d, J = 8.2 Hz, 2H), 6.88 (dd, J = 2.7, 3.9 Hz, 1H), 6.76−6.72 (m, 1H), 6.16 (dd, J = 2.8, 6.0 Hz, 1H), 6.10−6.06 (m, 1H), 5.96−5.92 (m, 1H), 5.59 (s, 1H), 3.90 (s, 3H); ^{13}C NMR ($CDCl_3$, 100 Hz), 178.8, 166.7, 145.7, 142.0, 132.4, 130.0, 129.7, 129.2, 128.3, 122.5, 118.3, 111.0, 108.6, 108.2, 52.2, 44.0; ESI-MS: Calcd: 309.1234, Obsd: 309.1239 ($[M + H]^+$, M = $C_{18}H_{16}N_2O_3$); Anal. Calcd for $C_{18}H_{16}N_2O_3$: C, 70.12; H, 5.23; N, 9.09. Found: C, 69.85; H, 5.27; N, 9.01.

13-Bromo-10-(4-(methoxycarbonyl)phenyl)-17,17-dimethylchlorin (C-Br). Following a reported procedure,[44] a solution of **2** (1.08 g, 3.51 mmol) in THF (40 mL) was treated with NBS (1.32 g, 7.36 mmol) at −78 °C. After 1 h, the cooling bath was removed, the reaction mixture was allowed to warm to −20 °C, and a mixture of hexane and water (1:1, 10 mL) was added. The resulting mixture was diluted with ethyl acetate, washed with brine, dried (Na_2SO_4), and concentrated. Column chromatography [hexane/ethyl acetate (1:1)] provides the semipure 8,9-dibromo-1-formyl-5-(4-(methoxycarbonyl)-phenyl)dipyrromethane (**3**), as a yellow solid (1.63 g, 100%), which was used immediately in next step without further purification. ^{1}H NMR δ ($CDCl_3$, 400 MHz) 3.92 (s, 3H), 5.49 (s, 1H), 5.96 (s, 1H), 6.13 (s, 1H), 6.93 (d, J = 4.0 Hz, 1H), 7.23 (d, J = 8.4 Hz, 2H), 7.99 (d, J = 8.4 Hz, 2H), 8.54 (br, 1H), 9.33 (s, 1H), 9.65 (br, 1H).

Following a reported procedure,[24] a suspension of 3,4,5,6-tetrahydro-1,3,3-trimethyldipyrrin **4** (0.68 g, 3.6 mmol) and 8,9-dibromo-1-formyl-5-(4-(methoxycarbonyl)phenyl)dipyrromethane (1.63 g, 3.5 mmol) in dichloromethane (100 mL) was treated with a solution of *p*-toluenesulfonic acid (3.4 g, 18 mmol) in methanol (24 mL) and stirred at room temperature for 40 min. The resulting mixture was treated with 2,2,6,6-tetramethylpiperidine (6.60 mL, 38.9

dx.doi.org/10.1021/jo4016858 | J. Org. Chem. 2013, 78, 10678−10691

mmol). The reaction mixture was concentrated, and resulting brown solid was suspended in acetonitrile (360 mL) and treated with zinc acetate (9.7 g, 52 mmol), 2,2,6,6-tetramethylpiperidine (15 mL, 89 mmol), and silver trifluoromethanesulfonate (2.7 g, 11 mmol). The resulting suspension was refluxed for 18 h. The reaction mixture was cooled and concentrated, and the residue was purified by silica column chromatography (dichloromethane). The resulting green solid (crude zinc chlorin, 0.31 g) was treated with a solution of TFA (4 mL, 52 mmol) in CH_2Cl_2 (50 mL). The resulting mixture was stirred for 3 h, washed (saturated aqueous $NaHCO_3$ and water), dried (Na_2SO_4), and concentrated. Column chromatography [silica, hexane/CH_2Cl_2 (1:2)] provides **C-Br** as a green solid (0.20 g, 10%). ^{1}H NMR ($CDCl_3$, 400 MHz) δ −2.28 (s, 1H), −1.92 (s, 1H), 2.07 (s, 6H), 4.12 (s, 3H), 4.69 (s, 2H), 8.21 (d, J = 8.6 Hz, 2H), 8.42 (d, J = 8.6 Hz, 2H), 8.56 (d, J = 4.3 Hz, 1H), 8.79 (s, 1H), 8.92−8.99 (m, 3H), 9.20 (s, 1H), 9.24 (d, J = 4.9 Hz, 1H), 9.84 (s, 1H); ^{13}C NMR ($CDCl_3$, 100 MHz) δ 31.1, 46.5, 52.1, 52.4, 95.1, 95.2, 107.5, 112.8, 119.6, 124.0, 128.0, 128.1, 128.8, 129.6, 132.1, 132.85, 132.91, 134.0, 134.9, 136.1, 141.4, 146.0, 151.5, 152.0, 163.4, 167.3, 176.0; MS ([M + H]$^+$, M = $C_{30}H_{25}BrN_4O_2$): Calcd: 553.1234, Obsd: (MALDI-MS) 552.9, (HRMS-ESI) 553.1234.

13-(4-Aminophenyl)-10-(4-(methoxycarbonyl)phenyl)-17,17-dimethylchlorin (C-NH$_2$). A mixture of **C-Br** (28 mg, 51 μmol), 4-aminophenylboronic acid pinacol ester (22 mg, 100 μmol), potassium carbonate (13.8 mg, 100 μmol), and tetrakis-(triphenylphosphine)palladium (12 mg, 10 μmol) in toluene (6 mL) and DMF (3 mL) was stirred at 100 °C under nitrogen. After 14 h, the mixture was diluted with ethyl acetate, washed (water and brine), dried (Na_2SO_4), and concentrated. A residue was purified by silica column chromatography (ethyl acetate and CH_2Cl_2 (1:40)) to afford a green powder (**C-NH$_2$**, 22 mg, 77%). ^{1}H NMR ($CDCl_3$, 400 MHz) δ −2.18 (s, 1H), −1.99 (s, 1H), 2.07 (s, 6H), 3.92 (s, 2H), 4.11 (s, 3H), 4.64 (s, 2H), 7.03 (d, J = 8.0 Hz, 2H), 7.95 (d, J = 7.9 Hz, 2H), 8.27 (d, J = 8.0 Hz, 2H), 8.42 (d, J = 7.9 Hz, 2H), 8.58 (d, J = 4.3 Hz, 1H), 8.70 (s, 1H), 8.89−8.98 (m, 2H), 9.00 (d, J = 4.3 Hz, 1H), 9.20 (s, 1H), 9.24 (d, J = 4.3 Hz, 1H), 9.87 (s, 1H); ^{13}C NMR ($CDCl_3$, 100 MHz) δ 31.2, 46.3, 52.3, 52.6, 94.7, 96.1, 107.5, 115.5, 119.0, 122.9, 125.4, 126.1, 127.9, 128.0, 129.4, 131.5, 132.4, 132.7, 133.8, 134.2, 137.9, 138.3, 140.7, 146.4, 147.0, 150.9, 152.5, 163.5, 167.4, 174.9; MS ([M + H]$^+$, M = $C_{36}H_{31}N_5O_2$): Calcd: 566.2551, Obsd: (MALDI-MS) 566.0, (HRMS-ESI) 566.2546; λ_{abs} (toluene) = 413, 504, 646 nm.

3-Bromo-5-methoxy-13-(4-(methoxycarbonyl)phenyl)-8,8,18,18-tetramethylbacteriochlorin (BC-BrCOOMe). A mixture of 3,13-dibromo-5-methoxy-8,8,18,18-tetramethylbacteriochlorin **BC-Br$_2$**[48] (167 mg, 0.299 mmol), 4-(methoxycarbonyl)phenylboronic acid pinacol ester (86 mg, 0.33 mmol), potassium carbonate (414 mg, 3.00 mmol), and tetrakis(triphenylphosphine)palladium (34 mg, 0.030 mmol) in toluene (40 mL) and DMF (20 mL) was stirred at 80−90 °C under nitrogen. After 18 h, the mixture was diluted with ethyl acetate, washed (water and brine), dried (Na_2SO_4), and concentrated. A residue was purified with silica column chromatography (hexane and CH_2Cl_2 (1:2)) to afford a green powder (**BC-BrCOOMe**, 136 mg, 74%). ^{1}H NMR ($CDCl_3$, 400 MHz) δ −1.79 (s, 1H), −1.52 (s, 1H), 1.92 (s, 6H), 1.97 (s, 6H), 4.06 (s, 3H), 4.36 (s, 5H), 4.43 (s, 2H), 8.23 (d, J = 7.9 Hz, 2H), 8.41 (d, J = 7.9 Hz, 2H), 8.51 (s, 1H), 8.63 (s, 1H), 8.69 (d, J = 1.8 Hz, 1H), 8.73 (s, 1H), 8.80 (s, 1H); ^{13}C NMR ($CDCl_3$, 100 MHz) δ 30.8, 31.1, 45.4, 45.9, 47.2, 52.0, 52.3, 64.4, 96.7, 97.2, 104.7, 123.0, 123.7, 126.3, 129.1, 130.2, 130.8, 133.6, 135.4, 135.6, 135.7, 135.8, 140.8, 153.9, 161.5, 167.2, 169.1, 170.4; MS ([M + H]$^+$, M = $C_{33}H_{33}BrN_4O_3$): Calcd: 613.1809, Obsd: (MALDI-MS) 613.1, (HRMS-ESI) 613.1833.

5-Methoxy-13-(4-(methoxycarbonyl)phenyl-8,8,18,18-tetramethylbacteriochlorin (BC1). A mixture of **BC-BrCOOMe** (18.2 mg, 0.030 mmol), potassium carbonate (41 mg, 0.30 mmol), formic acid (10 μL, 0.30 mmol), and tetrakis(triphenylphosphine)palladium (3.4 mg, 30 μmol) in toluene (6 mL) and DMF (3 mL) was stirred at 80−90 °C under nitrogen. After 10 h, the mixture was diluted with ethyl acetate, washed (water and brine), dried (Na_2SO_4), and concentrated. A residue was purified with silica column chromatography (hexane and CH_2Cl_2 (1:2)) to afford a green powder (**BC1**, 14.7 mg, 93%). ^{1}H NMR ($CDCl_3$, 400 MHz) δ −2.12 (s, 1H), −1.93 (s, 1H), 1.97 (s, 6H), 2.00 (s, 6H), 4.07 (s, 3H), 4.42 (s, 2H), 4.44 (s, 2H), 4.51 (s, 3H), 8.28 (d, J = 7.3 Hz, 2H), 8.41 (d, J = 8.0 Hz, 2H), 8.69 (s, 1H), 8.72 (s, 2H), 8.84 (s, 2H), 8.97 (d, J = 4.3 Hz, 1H); ^{13}C NMR ($CDCl_3$, 100 MHz) δ 31.0, 31.1, 45.6, 45.7, 47.7, 51.9, 52.3, 65.2, 96.5, 96.9, 97.0, 118.0, 120.9, 121.6, 128.8, 130.1, 131.0, 131.5, 133.9, 134.3, 134.7, 135.2, 136.1, 141.4, 153.9, 159.5, 167.3, 169.1, 169.6; MS ([M + H]$^+$, M = $C_{33}H_{34}N_4O_3$): Calcd: 535.2704, Obsd: (MALDI-MS) 534.9, (HRMS-ESI) 535.2699.

3-(4-(Dimethylamino)phenylethynyl)-5-methoxy-13-(4-(methoxycarbonyl)phenyl)-8,8,18,18-tetramethylbacteriochlorin (BC2). A mixture of **BC-BrCOOMe** (20.2 mg, 33 μmol), 4-ethynyl-*N*,*N*-dimethylaniline (9.6 mg, 66 μmol), and bis-(triphenylphosphine)palladium dichloride (2.3 mg, 3.0 μmol) in triethylamine (2.5 mL) and DMF (5 mL) was stirred at 80−90 °C under nitrogen. After 5 h, the mixture was diluted with ethyl acetate, washed, (water and brine), dried (Na_2SO_4), and concentrated. A residue was purified with silica column chromatography (hexane and CH_2Cl_2 (1:4)) to afford a brown-red solid (**BC2**, 17.2 mg, 77%). ^{1}H NMR ($CDCl_3$, 400 MHz) δ −1.81 (s, 1H), −1.49 (s, 1H), 1.94 (s, 6H), 1.97 (s, 6H), 3.07 (s, 6H), 4.06 (s, 3H), 4.36 (s, 2H), 4.47 (s, 2H), 4.53 (s, 3H), 6.82 (d, J = 8.6 Hz, 2H), 7.76 (d, J = 8.6 Hz, 2H), 8.25 (d, J = 8.0 Hz, 2H), 8.41 (d, J = 8.0 Hz, 2H), 8.55 (s, 1H), 8.63 (s, 1H), 8.74 (s, 1H), 8.76−8.83 (m, 2H); ^{13}C NMR ($CDCl_3$, 100 MHz) δ 30.9, 31.0, 40.3, 45.4, 45.7, 47.5, 52.0, 52.3, 64.4, 85.3, 95.0, 96.6, 96.8, 97.1, 111.3, 112.0, 113.5, 122.3, 123.8, 128.9, 130.2, 130.9, 131.2, 132.8, 134.4, 134.89, 134.98, 135.4, 135.6, 141.1, 150.1, 154.6, 160.7, 167.2, 169.3, 169.9; MS ([M + H]$^+$, M = $C_{43}H_{43}N_5O_3$): Calcd: 678.3439, Obsd: (MALDI-MS) 677.8, (HRMS-ESI) 678.3419.

3-[(*Z*)-2,4-Diphenylbut-1-en-3-yn-1-yl]-5-methoxy-13-(4-(methoxycarbonyl)phenylethynyl)-8,8,18,18-tetramethylbacteriochlorin (BC5). Synthetic procedure and ^{1}H NMR and HRMS data have been presented elsewhere.[47] ^{13}C NMR ($CDCl_3$, 100 MHz) δ 30.9, 31.0, 45.1, 45.9, 48.2, 51.3, 52.3, 64.1, 88.2, 90.2, 95.3, 96.4, 97.1, 97.7, 108.7, 114.5, 121.4, 122.4, 123.9, 124.0, 126.5, 127.9, 128.55, 128.64, 128.7, 129.5, 129.6, 129.7, 130.2, 130.6, 131.6, 131.8, 134.6, 135.9, 136.3, 137.5, 139.6, 156.7, 160.2, 166.7, 169.2, 170.9.

Dyad C-BC1. A mixture of **BC1** (11.2 mg, 21.0 μmol), aqueous NaOH (2 mL, 1 M), THF (4 mL), and methanol (2 mL) was stirred at room temperature for 15 h. HCl solution (1 M, 10 mL) was added, and the resulting mixture was extracted with ethyl acetate. Combined organic layers were washed with brine, dried (Na_2SO_4), and concentrated. The resulting crude solid (11.0 mg, 100%) was suspended in DMF (1 mL) and treated with DMAP (24.4 mg, 200 μmol), **C-NH$_2$** (12 mg, 21 μmol), and EDCI (38 mg, 200 μmol). The resulting mixture was stirred at room temperature. After 14 h, the mixture was diluted with ethyl acetate, washed with brine, dried (Na_2SO_4), and concentrated. A residue was purified with silica column chromatography (CH_2Cl_2 and ethyl acetate (40:1)) to afford a green solid (**C-BC1**, 13.9 mg, 62%). ^{1}H NMR ($CDCl_3$, 400 Hz) δ −2.16 (s, 1H), −2.10 (s, 1H), −1.90 (s, 2H), 1.98 (s, 6H), 2.01 (s, 6H), 2.09 (s, 6H), 4.13 (s, 3H), 4.44 (s, 2H), 4.46 (s, 2H), 4.53 (s, 3H), 4.67 (s, 2H), 8.10 (d, J = 8.6 Hz, 2H), 8.21 (d, J = 7.9 Hz, 2H), 8.25 (s, 1H), 8.29−8.35 (m, 6H), 8.46 (d, J = 8.6 Hz, 2H), 8.61 (d, J = 4.3 Hz, 1H), 8.71 (s, 1H), 8.72−8.76 (m, 2H), 8.82 (s, 1H), 8.85 (d, J = 1.8 Hz, 1H), 8.87 (s, 1H), 8.95−9.01 (m, 4H), 9.24 (d, J = 4.9 Hz, 1H), 9.26 (s, 1H), 9.87 (s, 1H); ^{13}C NMR ($CDCl_3$, 100 MHz) δ 31.06, 31.1, 31.2, 45.68, 45.7, 46.4, 47.7, 51.9, 52.4, 65.3, 94.8, 95.9, 96.5, 96.9, 97.0, 107.4, 118.1, 119.6, 120.7, 121.1, 121.5, 123.4, 125.9, 127.7, 128.1, 128.3, 129.4, 131.4, 131.6, 131.8, 132.1, 132.3, 132.8, 133.32, 133.35, 133.8, 134.0, 134.2, 134.4, 134.7, 135.2, 136.1, 137.0, 137.3, 137.7, 140.6, 140.9, 146.8, 151.2, 152.3, 154.0, 159.4, 163.6, 165.8, 167.4, 169.1, 169.7, 175.4; MS ([M + H]$^+$, M = $C_{68}H_{61}N_9O_4$): Calcd: 1068.4919, Obsd: (MALDI-MS) 1068.1, (HRMS-ESI) 1068.4936.

Dyad C-BC2. A mixture of **BC2** (13.5 mg, 19.9 μmol), aqueous NaOH (2 mL, 1 M), THF (4 mL), and methanol (2 mL) was stirred at room temperature for 15 h. HCl solution (1 M, 10 mL) was added, and the resulting mixture was extracted with ethyl acetate. Combined organic layers were washed with brine, dried (Na_2SO_4), and concentrated. The resulting crude solid was suspended in DMF (1

dx.doi.org/10.1021/jo4016858 | J. Org. Chem. 2013, 78, 10678−10691

mL) and treated with DMAP (24 mg, 200 μmol), **C-NH$_2$** (11.3 mg, 20.0 μmol), and EDCI (38 mg, 200 μmol). The resulting mixture was stirred at room temperature. After 16 h, the mixture was diluted with ethyl acetate, washed with brine, dried (Na_2SO_4), and concentrated. A residue was purified with silica column chromatography (CH_2Cl_2 and ethyl acetate (50:1)) to afford a green solid (**C-BC2**, 14.6 mg, 60%). ^{1}H NMR ($CDCl_3$, 400 MHz) δ −2.17 (s, 1H), −1.91 (s, 1H), −1.80 (s, 1H), −1.48 (s, 1H), 1.96 (s, 6H), 1.99 (s, 6H), 2.10 (s, 6H), 3.06 (s, 6H), 4.12 (s, 3H), 4.39 (s, 2H), 4.49 (s, 2H), 4.54 (s, 3H), 4.68 (s, 2H), 6.80 (d, J = 9.2 Hz, 2H), 7.75 (d, J = 8.6 Hz, 2H), 8.11 (d, J = 7.9 Hz, 2H), 8.22 (d, J = 8.6 Hz, 2H), 8.23 (s, 1H), 8.28−8.34 (m, 6H), 8.45 (d, J = 8.0 Hz, 2H), 8.57 (s, 1H), 8.60 (d, J = 4.3 Hz, 1H), 8.66 (s, 1H), 8.76 (s, 1H), 8.78−8.83 (m, 3H), 8.95−9.02 (m, 3H), 9.23−9.27 (m, 2H), 9.89 (s, 1H); ^{13}C NMR ($CDCl_3$, 100 MHz) δ 30.9, 31.1, 31.2, 40.3, 45.5, 45.7, 46.4, 47.5, 52.0, 52.4, 64.5, 85.2, 94.8, 95.1, 95.9, 96.5, 96.8, 97.2, 107.4, 111.2, 112.0, 113.7, 119.6, 120.7, 122.2, 123.4, 123.9, 125.9, 127.7, 128.1, 128.3, 129.4, 131.27, 131.32, 131.8, 132.1, 132.3, 132.77, 132.85, 133.4, 133.5, 134.2, 134.4, 134.5, 134.7, 134.8, 135.4, 135.6, 136.9, 137.3, 137.7, 140.3, 140.9, 146.8, 150.1, 151.2, 152.3, 154.7, 160.7, 163.6, 165.7, 167.4, 169.4, 169.9, 175.4; MS ([M + H]$^+$, M = $C_{78}H_{70}N_{10}O_4$): Calcd: 1211.5654, Obsd: (MALDI-MS) 1211.2, (HRMS-ESI) 1211.5699.

Dyad C-BC3. A mixture of **BC3** (14 mg, 24 μmol), aqueous NaOH (2 mL, 1 M), THF (4 mL), and methanol (2 mL) was stirred at room temperature for 12 h. HCl solution (1 M, 10 mL) was added, and the resulting mixture was extracted with ethyl acetate. Combined organic layers were washed with brine, dried (Na_2SO_4), and concentrated. The resulting crude solid (14 mg, 100%) was suspended in DMF (1 mL) and treated with DMAP (30 mg, 240 μmol), **C-NH$_2$** (13.6 mg, 24 μmol), and EDCI (47 mg, 240 μmol). The resulting mixture was stirred at room temperature. After 16 h, the mixture was diluted with ethyl acetate, washed with brine, dried (Na_2SO_4), and concentrated. A residue was purified with silica column chromatography (CH_2Cl_2 and ethyl acetate (40:1)) to afford a green solid (**C-BC3**, 12.6 mg, 48%). ^{1}H NMR ($CDCl_3$, 400 MHz) δ −2.18 (s, 1H), −1.94 (s, 1H), −1.92 (s, 1H), −1.57 (s, 1H), 1.971 (s, 6H), 1.975 (s, 6H), 2.09 (s, 6H), 4.12 (s, 3H), 4.27 (s, 3H), 4.43 (s, 2H), 4.47 (s, 2H), 4.67 (s, 2H), 5.77 (d, J = 12.2 Hz, 1H), 6.38 (d, J = 17.2 Hz, 1H), 8.07 (t, J = 9.2 Hz, 4H), 8.14 (d, J = 8.5 Hz, 3H), 8.21 (d, J = 8.6 Hz, 2H), 8.29 (d, J = 8.5 Hz, 2H), 8.38−8.47 (m, 3H), 8.57−8.62 (m, 3H), 8.79 (s, 1H), 8.81 (d, J = 1.8 Hz, 1H), 8.83 (d, J = 1.8 Hz, 1H), 8.94−8.92 (m, 4H), 9.23 (s, 1H), 9.26 (d, J = 4.9 Hz, 1H), 9.88 (s, 1H); ^{13}C NMR (THF-d_8, 100 MHz) δ 31.0, 31.2, 31.4, 45.9, 46.8, 47.2, 49.0, 52.0, 52.4, 53.1, 64.4, 79.0, 79.3, 79.6, 88.3, 95.7, 96.0, 96.7, 96.9, 97.4, 98.7, 108.2, 115.1, 116.7, 119.7, 120.3, 121.3, 121.4, 124.2, 124.4, 126.4, 128.0, 128.8, 129.0, 130.0, 130.7, 132.3, 132.4, 132.5, 133.4, 133.7, 134.4, 135.1, 135.4, 136.1, 137.1, 137.6, 140.5, 141.8, 142.0, 147.9, 152.5, 153.4, 157.4, 160.6, 164.4, 165.6, 167.3, 169.5, 171.9, 176.1. Note: Because of low solubility of **C-BC3** in $CDCl_3$, ^{13}C NMR spectra were collected in THF-d_8. ^{1}H NMR spectra were reported in $CDCl_3$, due to the better peak resolution in that solvent, compared to THF-d_8. MS ([M + H]$^+$, M = $C_{72}H_{63}N_9O_4$): Calcd: 1118.5076, Obsd: (MALDI-MS) 1118.7, (HRMS-ESI) 1118.5117.

Dyad C-BC4. A mixture of **BC4** (9.1 mg, 14 μmol), aqueous NaOH (2 mL, 1 M), THF (4 mL), and methanol (2 mL) was stirred at room temperature for 16 h. HCl solution (1 M, 10 mL) was added, and the resulting mixture was extracted with ethyl acetate. Combined organic layers were washed with brine, dried (Na_2SO_4), and concentrated. The resulting crude solid (9.1 mg, 100%) was suspended in DMF (1 mL) and treated with DMAP (17 mg, 140 μmol), **C-NH$_2$** (7.9 mg, 14 μmol), and EDCI (27 mg, 140 μmol). The resulting mixture was stirred at room temperature. After 16 h, the mixture was diluted with ethyl acetate, washed with brine, dried (Na_2SO_4), and concentrated. A residue was purified with silica column chromatography (CH_2Cl_2 and ethyl acetate (50:1)) to afford a green solid (**C-BC4**, 6.5 mg, 40%). ^{1}H NMR ($CDCl_3$, 400 MHz) δ −2.12 (s, 1H), −1.87 (s, 1H), −1.71 (s, 1H), −1.45 (s, 1H), 1.98 (s, 12H), 2.10 (s, 6H), 4.12 (s, 3H), 4.46 (s, 4H), 4.52 (s, 3H), 4.67 (s, 2H), 7.41−7.53 (m, 3H), 7.87 (d, J = 7.4 Hz, 2H), 8.02−8.11 (m, 5H), 8.14 (d, J = 8.0 Hz, 2H), 8.20 (d, J = 7.9 Hz, 2H), 8.29 (d, J = 7.9 Hz, 2H), 8.44 (d, J = 7.9 Hz, 2H), 8.53−8.61 (m, 3H), 8.77−8.86 (m, 3H), 8.92−9.01 (m, 4H), 9.19−9.27 (m, 2H), 9.87 (s, 1H); MS ([M + H]$^+$, M = $C_{78}H_{65}N_9O_4$): Calcd: 1192.5232, Obsd: (MALDI-MS) 1191.8, (HRMS-ESI) 1192.5276.

Dyad C-BC5. A mixture of **BC5** (14.8 mg, 19.4 μmol), aqueous NaOH (2 mL, 1 M), THF (4 mL), and methanol (2 mL) was stirred at room temperature for 9 h. HCl solution (1 M, 10 mL) was added, and the resulting mixture was extracted with ethyl acetate. Combined organic layers were washed with brine, dried (Na_2SO_4), and concentrated. The resulting crude solid (13.2 mg, 91%) was suspended in DMF (1 mL) and treated with DMAP (24 mg, 197 μmol), **C-NH$_2$** (11 mg, 19.4 μmol), and EDCI (38 mg, 200 μmol). The resulting mixture was stirred at room temperature. After 18 h, the mixture was diluted with ethyl acetate, washed with brine, dried (Na_2SO_4), and concentrated. A residue was purified with silica column chromatography (CH_2Cl_2) to afford a red solid (**C-BC5**, 16.6 mg, 73%). ^{1}H NMR ($CDCl_3$, 400 MHz) δ −2.17 (s, 1H), −1.93 (s, 1H), −1.71 (s, 1H), −1.40 (s, 1H), 1.99 (s, 12H), 2.09 (s, 6H), 4.12 (s, 3H), 4.30 (s, 3H), 4.45 (s, 2H), 4.47 (s, 2H), 4.67 (s, 2H), 7.41−7.60 (m, 6H), 7.84 (d, J = 6.7 Hz, 2H), 7.95−8.13 (m, 7H), 8.17 (d, J = 7.9 Hz, 4H), 8.30 (d, J = 8.0 Hz, 2H), 8.46 (d, J = 8.0 Hz, 2H), 8.56−8.65 (m, 3H), 8.80 (s, 1H), 8.84 (s, 1H), 8.93−9.02 (m, 4H), 9.20−9.31 (m, 3H), 9.79 (s, 1H), 9.89 (s, 1H); MS ([M + H]$^+$, M = $C_{86}H_{71}N_9O_4$): Calcd: 1294.5702, Obsd: 1293.9 (MALDI-MS), 1294.5652 (HRMS-ESI).

C-BC1-NHS. A mixture of **C-BC1** (10.8 mg, 10.1 μmol), aqueous NaOH (2 mL, 1 M), THF (4 mL), and methanol (2 mL) was stirred at room temperature for 13 h. HCl solution (1 M, 10 mL) was added. The resulting mixture was extracted with ethyl acetate. Combined organic layers were washed with brine, dried (Na_2SO_4), and concentrated. The resulting crude solid (10.3 mg, 97%) was suspended in DMF (1 mL) and treated with DMAP (12.2 mg, 100 μmol), *N*-hydroxysuccinimide (11.5 mg, 100 μmol), and EDCI (19 mg, 100 μmol). After 15 h, the mixture was diluted with ethyl acetate, washed with brine, dried (Na_2SO_4), and concentrated. A residue was purified with silica column chromatography (CH_2Cl_2 and ethyl acetate (50:1)) to afford a green solid (**C-BC1-NHS**, 8.3 mg, 74%). ^{1}H NMR ($CDCl_3$, 400 MHz) δ −2.20 (s, 1H), −2.11 (s, 1H), −1.97 (s, 1H), −1.91 (s, 1H), 1.98 (s, 6H), 2.01 (s, 6H), 2.09 (s, 6H), 3.00 (br, 4H), 4.45 (s, 4H), 4.52 (s, 3H), 4.68 (s, 2H), 8.09−8.19 (m, 2H), 8.22−8.41 (m, 9H), 8.55 (d, J = 7.3 Hz, 3H), 8.67−8.77 (m, 3H), 8.80 (s, 1H), 8.88 (s, 2H), 8.99 (s, 4H), 9.25 (s, 1H), 9.30 (s, 1H), 9.91 (s, 1H); MS ([M + H]$^+$, M = $C_{71}H_{62}N_{10}O_6$): Calcd: 1151.4927, Obsd: 1151.4970 (HRMS-ESI); λ_{abs} (toluene) = 368, 414, 506, 647, 724 nm.

C-BC2-NHS. A mixture of **C-BC2** (5.7 mg, 4.7 μmol), aqueous NaOH (2 mL, 1 M), THF (4 mL), and methanol (2 mL) was stirred at room temperature for 10 h. HCl solution (1 M, 10 mL) was added, and the resulting mixture was extracted with ethyl acetate. Combined organic layers were washed with brine, dried (Na_2SO_4), and concentrated. The resulting crude solid (5.9 mg, 100%) was suspended in DMF (1 mL) and treated with DMAP (5.7 mg, 47 μmol), *N*-hydroxysuccinimide (5.4 mg, 47 μmol), and EDCI (8.9 mg, 47 μmol). The resulting mixture was stirred at room temperature. After 16 h, the mixture was diluted with ethyl acetate, washed with brine, dried (Na_2SO_4), and concentrated. A residue was purified with silica column chromatography (CH_2Cl_2 and ethyl acetate (15:1)) to afford a violet-brown solid (**C-BC2-NHS**, 3.4 mg, 56%). ^{1}H NMR ($CDCl_3$, 400 MHz) δ −2.19 (s, 1H), −1.95 (s, 1H), −1.79 (s, 1H), −1.46 (s, 1H), 1.96 (s, 6H), 1.99 (s, 6H), 2.10 (s, 6H), 3.02 (br, 4H), 3.08 (s, 6H), 4.39 (s, 2H), 4.48 (s, 2H), 4.53 (s, 3H), 4.69 (s, 2H), 6.85 (br, 2H), 7.76 (d, J = 7.9 Hz, 2H), 8.12−8.20 (m, 2H), 8.26 (d, J = 8.0 Hz, 3H), 8.32−8.41 (m, 6H), 8.52−8.59 (m, 4H), 8.66 (s, 1H), 8.74−8.85 (m, 4H), 8.97−9.06 (m, 3H), 9.24−9.31 (m, 2H), 9.91 (s, 1H); MS ([M + H]$^+$, M = $C_{81}H_{71}N_{11}O_6$): Calcd: 1294.5662, Obsd: 1294.5645 (HRMS-ESI); λ_{abs} (toluene) = 370, 414, 521, 647, 749 nm.

C-BC5-NHS. A mixture of **C-BC5** (14.1 mg, 10.9 μmol), aqueous NaOH (2 mL, 1 M), THF (4 mL), and methanol (2 mL) was stirred at room temperature for 9 h. HCl solution (1 M, 10 mL) was added, and the resulting mixture was extracted with ethyl acetate. Combined organic layers were washed with brine, dried (Na_2SO_4), and concentrated. The resulting crude solid (13.9 mg, 100%) was

dx.doi.org/10.1021/jo4016858 | J. Org. Chem. 2013, 78, 10678−10691

suspended in DMF (1 mL) and treated with DMAP (13.4 mg, 110 μmol), *N*-hydroxysuccinimide (12.7 mg, 110 μmol), and EDCI (20.9 mg, 110 μmol). The resulting mixture was stirred at room temperature. After 15 h, the mixture was diluted with ethyl acetate, washed with brine, and dried over Na_2SO_4. After being concentrated, the residue was purified with silica column chromatography (CH_2Cl_2 and ethyl acetate (25:1)) to afford a red solid (**C-BC5-NHS**, 6.5 mg, 43%). ^{1}H NMR ($CDCl_3$, 400 MHz) δ −2.20 (s, 1H), −1.98 (s, 1H), −1.71 (s, 1H), −1.41 (m, 1H), 1.99 (s, 12H), 2.10 (s, 6H), 3.02 (br, 4H), 4.30 (s, 3H), 4.44 (s, 2H), 4.47 (s, 2H), 4.68 (s, 2H), 7.41−7.62 (m, 6H), 7.84 (d, J = 8.0 Hz, 2H), 8.00−8.28 (m, 11H), 8.37 (d, J = 7.9 Hz, 2H), 8.51−8.66 (m, 5H), 8.79 (s, 1H), 8.84 (s, 1H), 8.93−9.07 (m, 4H), 9.23−9.32 (m, 3H), 9.78 (s, 1H), 9.92 (s, 1H); MS ([M + H]$^+$, M = $C_{89}H_{72}N_{10}O_6$): Calcd: 1377.5709, Obsd: 1377.5738 (HRMS-ESI) .

Amide C-NHPh. A mixture of **C-NH$_2$** (6.7 mg, 12 μmol), DMAP (2.9 mg, 24 μmol), and benzoic acid (2.9 mg, 24 μmol) in DMF (2 mL) was treated with EDCI (4.6 mg, 24 μmol). The resulting mixture was stirred at room temperature. After 16 h, the mixture was diluted with ethyl acetate, washed with brine, dried (Na_2SO_4), and concentrated. A residue was purified with silica column chromatography (CH_2Cl_2 and ethyl acetate (40:1)) to afford a green solid (**C-NHPh**, 6.9 mg, 87%). ^{1}H NMR ($CDCl_3$, 400 MHz) δ −2.19 (s, 1H), −1.95 (s, 1H), 2.07 (s, 6H), 4.11 (s, 3H), 4.64 (s, 2H), 7.54−7.65 (m, 3H), 7.97−8.07 (m, 5H), 8.15 (d, J = 8.6 Hz, 2H), 8.27 (d, J = 7.9 Hz, 2H), 8.42 (d, J = 8.6 Hz, 2H), 8.58 (d, J = 4.3 Hz, 1H), 8.76 (s, 1H), 8.93−9.01 (m, 3H), 9.20 (s, 1H), 9.25 (d, J = 4.9 Hz, 1H), 9.87 (s, 1H); ^{13}C NMR ($CDCl_3$, 100 MHz) δ 31.2, 46.4, 52.4, 94.8, 96.0, 107.4, 119.5, 120.6, 123.4, 125.9, 127.1, 128.1, 128.3, 128.9, 129.4, 131.7, 132.0, 132.2, 132.6, 133.3, 134.1, 134.4, 134.9, 137.0, 137.4, 137.6, 140.9, 146.8, 163.6, 165.9, 167.4, 175.4; MS ([M + H]$^+$, M = $C_{43}H_{35}N_5O_3$): Calcd: 670.28127, Obsd: 670.3, (MALDI-MS) 670.2794 (HRMS-ESI).

■ ASSOCIATED CONTENT

Supporting Information

Comparison of ^{1}H NMR spectra of selected dyad and corresponding benchmark monomers, additional absorption spectra, ORTEP view and details of X-ray analysis for compound **BC5**, copies of NMR spectra for new compounds, and CIF file for **BC5**. This material is available free of charge via the Internet at http://pubs.acs.org.

■ AUTHOR INFORMATION

Corresponding Author

*E-mail: mptaszek@umbc.edu.

Notes

The authors declare no competing financial interest.

■ ACKNOWLEDGMENTS

Authors thank Dr. Dewey Holten for a valuable discussion. X-ray data were collected at the X-ray facility of the Department of Chemistry at the Johns Hopkins University. Authors thank Dr. Maxime A. Siegler for his contribution to the X-ray structure determination of compound **BC5**. This work was supported by University of Maryland, Baltimore County (start-up funds and SRAIS award).

■ REFERENCES

(1) Kobayashi, H.; Ogawa, M.; Choyke, Alford, R.; Choyke, P. L.; Urano, Y. *Chem. Rev.* **2010**, *110*, 2620−2640.
(2) Kobayashi, H.; Longmire, M. R.; Ogawa, M.; Choyke, P. L. *Chem. Soc. Rev.* **2011**, *40*, 4626−4648.
(3) Kobayashi, H.; Hama, Y.; Koyama, Y.; Barrett, T.; Regino, C. A. S.; Urano, Y.; Choyke, P. L. *Nano Lett.* **2007**, *7*, 1711−1716.
(4) Kobayashi, H.; Koyama, Y.; Barrett, T.; Hama, Y.; Regino, C. A. S.; Shin, I. S.; Jang, B.-S.; Le, W.; Paik, C. H.; Choyke, P. L.; Urano, Y. *ACS Nano* **2007**, *1*, 258−264.
(5) Koyama, Y.; Barrett, T.; Hama, Y.; Ravizzini, P. L.; Choyke, P. L.; Kobayashi, H. *Neoplasia* **2007**, *9*, 1021−1029.
(6) Smith, B. A.; Xie, B.-W.; van Beek, E. R.; Que, I.; Blankevoort, V.; Xiao, S.; Cole, E. L.; Hoehn, M.; Kaijzel, E. L.; Löwik, C. W. G. M.; Smith, B. D. *ACS Chem. Neurosci.* **2012**, *3*, 530−537.
(7) Yang, M.; Jiang, P.; Hoffman, R. M. *Cancer Res.* **2007**, *67*, 5195−5200.
(8) Shcherbakova, D. M.; Verkhusha, V. V. *Nat. Methods* **2013**, *10*, 751−754.
(9) Kobayashi, H.; Kosaka, N.; Ogawa, M.; Ogawa, M.; Morgan, N. Y.; Smith, P. D.; Murray, C. B.; Ye, X.; Collins, J.; Kumar, G. A.; Bell, H.; Choyke, P. L. *J. Mater. Chem.* **2009**, *19*, 6481−6484.
(10) Cheng, L.; Yang, K.; Shao, M.; Lee, S.-T.; Liu, Z. *J. Phys. Chem. C* **2011**, *115*, 2686−2692.
(11) Resch-Genger, U.; Grabolle, M.; Cavaliere-Jaricot, S.; Nitschke, R.; Nann, T. *Nat. Methods* **2008**, *5*, 763−775.
(12) Tsoi, K. M.; Dai, Q.; Alman, B. A.; Chan, W. C. W. *Acc. Chem. Res.* **2013**, *46*, 662−671.
(13) (a) B. Grimm, B.; Porra, R. R.; Rüdiger, W.; Scheer, H., Eds. *Chlorophylls and Bacteriochlorophylls. Biochemistry, Biophysics, Function and Applications*; Springer: New York, 2006, Dodrecht. (b) Lindsey, J. S.; Mass, O.; Chen, C.-Y. *New J. Chem.* **2011**, *35*, 511−516. (c) Brückner, C.; Samankumara, L.; Ogikubo, J. In *Handbook of Porphyrin Sciences*; Kadish, K. M.; Smith, K. M.; Guilard, R., Eds.; World Scientific: River Edge, NY, 2012; Vol. *17*, pp 1−112.
(14) Tamiaki, H.; Kunieda, M. In *Handbook of Porphyrin Sciences*; Kadish, K. M.; Smith, K. M.; Guilard, R., Eds.; World Scientific Publishing,: London, 2011; Vol. *11*, pp 223−285.
(15) Yang, E.; Kirmaier, C.; Krayer, M.; Taniguchi, M.; Kim, H.-J.; Diers, J. R.; Bocian, D. F.; Lindsey, J. S.; Holten, D. *J. Phys. Chem. B* **2011**, *115*, 10801−10816.
(16) Kee, H. L.; Kirmaier, C.; Tang, Q.; Diers, J. R.; Muthiah, C.; Taniguchi, M.; Laha, J. K.; Ptaszek, M.; Lindsey, J. S.; Bocian, D. F.; Holten, D. *Photochem. Photobiol.* **2007**, *83*, 1125−1143.
(17) Taniguchi, M.; Cramer, D. L.; Bhise, A. D.; Kee, H. L.; Bocian, D. F.; Holten, D.; Lindsey, J. S. *New J. Chem.* **2008**, *32*, 947−958.
(18) Springer, J. W.; Faries, K. M.; Diers, J. R.; Muthiah, C.; Mass, O.; Kee, H. L.; Kirmaier, C.; Lindsey, J. S.; Bocian, D. F.; Holten, D. *Photochem. Photobiol.* **2012**, *88*, 651−674.
(19) Kee, H. L.; Kirmaier, C.; Tang, Q.; Diers, J. R.; Muthiah, C.; Taniguchi, M.; Laha, J. K.; Ptaszek, M.; Lindsey, J. S.; Bocian, D. F.; Holten, D. *Photochem. Photobiol.* **2007**, *83*, 1110−1124.
(20) Chen, C.-Y.; Sun, E.; Fan, M.; Taniguchi, M.; McDowell, B. E.; Yang, E.; Diers, J. R.; Bocian, D. F.; Holten, D.; Lindsey, J. S. *Inorg. Chem.* **2012**, *51*, 9443−9464.
(21) (a) Cao, W.; Ng, K. K.; Corbin, I.; Zhang, Z.; Ding, L.; Chen, J.; Zheng, G. *Bioconjugate Chem.* **2009**, *20*, 2023−2031. (b) Liu, T. W.; Akens, M. K.; Chen, J.; Wise-Milestone, L.; Wilson, B. C.; Zheng, G. *Bioconjugate Chem.* **2011**, *22*, 1021−1030. (c) Mawn, T. M.; Popov, A. V.; Beardsley, N. J.; Stefflova, K.; Milkevitch, M.; Zheng, G.; Delikatny, E. J. *Bioconjugate Chem.* **2011**, *22*, 2434−2443. (d) Popov, A. V.; Mawn, T. M.; Kim, S.; Zheng, G.; Delikatny, E. J. *Bioconjugate Chem.* **2010**, *21*, 1724−1727. (e) Vinita, A. M.; Sano, K.; Yu, Z.; Nakajima, T.; Choyke, P.; Ptaszek, M.; Kobayashi, H. *Bioconjugate Chem.* **2012**, *23*, 1671−1679.
(22) Liu, T. W. B.; Chen, J.; Burgess, L.; Cao, W.; Shi, J.; Wilson, B. C.; Zheng, G. *Theranostics* **2011**, *1*, 354−362.
(23) Lovell, J. F.; Jin, C. S.; Huynh, E.; Jin, H.; Kim, C.; Rubinstein, J. L.; Chan, W. C. W.; Cao, W.; Wang, L. V.; Zheng, G. *Nat. Mater.* **2011**, *10*, 324−332.
(24) Ptaszek, M.; Lahaye, D.; Krayer, M.; Muthiah, C.; Lindsey, J. S. *J. Org. Chem.* **2010**, *75*, 1659−1673.
(25) Sapsford, K., E.; Berti, L.; Medintz, I., L. *Angew. Chem., Int. Ed.* **2006**, *45*, 4562−4588.
(26) Fan, J.; Hu, M.; Zhan, P.; Peng, X. *Chem. Soc. Rev.* **2013**, *42*, 29−43.

(27) (a) Bandichhor, R.; Petrescu, A. D.; Vespa, A.; Kier, A. B.; Schroeder, F.; Burgess, K. *J. Am. Chem. Soc.* **2006**, *128*, 10688−10689. (b) Lin, W.; Yuan, L.; Cao, Z.; Feng, Y.; Song, J. *Angew. Chem., Int. Ed.* **2010**, *49*, 375−379. (c) Wu, L.; Loudet, A.; Barhoumi, R.; Burghardt, R. C.; Burgess, K. *J. Am. Chem. Soc.* **2009**, *131*, 9156−9157.
(28) Han, J.; Engler, A.; Qi, J.; Tung, C.-H. *Tetrahedron Lett.* **2013**, *54*, 502−505.
(29) Kee, H. L.; Nothdurft, R.; Muthiah, C.; Diers, J. R.; Fan, D.; Ptaszek, M.; Bocian, D. F.; Lindsey, J. S.; Culver, J. P.; Holten, D. *Photochem. Photobiol.* **2008**, *84*, 1061−1072.
(30) Guo, J.; Wang, S.; Dai, N.; Teo, Y. N.; Kool, E. T. *Proc. Natl. Acad. Sci. U.S.A.* **2011**, *108*, 3493−3498.
(31) Teo, Y. N.; Wilson, J. N.; Kool, E. T. *J. Am. Chem. Soc.* **2009**, *131*, 3923−3933.
(32) (a) Jiao, G.-S.; Thoresen, L. H.; Burgess, K. *J. Am. Chem. Soc.* **2003**, *125*, 14668−14669. (b) Rong, Y.; Wu, C.; Yu, J.; Zhang, X.; Ye, F.; Zeigler, M.; Gallina, M. E.; Wu, I.-C.; Zhang, Y.; Chan, Y.-H.; Sun, W.; Uvdal, K.; Chiu, D. T. *ACS Nano* **2013**, *7*, 376−384. (c) Ueno, Y.; Jose, J.; Loudet, A.; Pérez-Bolivar, C.; Anzenbacher, P., Jr.; Burgess, K. *J. Am. Chem. Soc.* **2011**, *133*, 51−55. (d) Thivierge, C.; Loudet, A.; Burgess, K. *Marcomolecules* **2011**, *44*, 4012−4015.
(33) Ptaszek, M.; Kee, H. L.; Muthiah, C.; Nothdurft, R.; Akers, W.; Achilefu, C.; Culver, J. P.; Holten, D. *SPIE-Int. Soc. Opt. Eng., Proc.* **2010**, *7576E*, 1−9.
(34) (a) Laakso, J.; Rosser, G. A.; Szijjártó, C.; Beeby, A.; Borbas, K. E. *Inorg. Chem.* **2012**, *51*, 10366−10374. (b) Redy, O.; Kisin-Finfer, E.; Sella, E.; Shabat, D. *Org. Biomol. Chem.* **2012**, *10*, 710−715. (c) Wiliams, M. P. A.; Ethirajan, M.; Ohkubo, K.; Chen, P.; Pera, P.; Morgan, J.; White, W. H., III; Shibata, M.; Fukuzumi, S.; Kadish, K. M.; Pandey, R. K. *Bioconjugate Chem.* **2011**, *22*, 2283−2295. (d) Oushiki, D.; Kojima, H.; Terai, T.; Arita, M.; Hanaoka, K.; Urano, Y.; Nagano, T. *J. Am. Chem. Soc.* **2010**, *132*, 2795−2801. (e) Kataoka, Y.; Shibata, Y.; Tamiaki, H. *Chem. Lett.* **2010**, *39*, 953−955. (f) Voznyak, D. A.; Zakharova, G. V.; Chibisov, A. K.; Kharitonova, O. V.; Grin, M. A.; Semenikhin, K. O.; Mironov, A. F. *High Energy Chem.* **2010**, *44*, 31−36. (g) Zhang, S.; Metelev, V.; Tabatadze, D.; Zamecnik, P. C.; Bogdanov, A., Jr. *Proc. Natl. Acad. Sci. U.S.A.* **2008**, *105*, 4156−4161. (h) Pham, W.; Choi, Y.; Weissleder, R.; Tung, C.-H. *Bioconjugate Chem.* **2004**, *15*, 1403−1407.
(35) (a) Harvey, P. D. In *Porphyrin Handbook*; Kadish, K. M.; Smith, K. M.; Guilard, R., Eds.; Academic Press: San Diego, 2003; Vol. *18*, pp 63−250. (b) Holten, D.; Bocian, D. F.; Lindsey, J. S. *Acc. Chem. Res.* **2002**, *35*, 57−69.
(36) (a) Miyatake, T.; Tamiaki, H.; Holzwarth, A. R.; Schaffner, K. *Photochem. Photobiol.* **1999**, *69*, 448−456. (b) Osuka, A.; Wada, Y.; Maruyama, K.; Tamiaki, H. *Heterocycles* **1997**, *44*, 165−168. (c) Tamiaki, H.; Miyatake, T.; Tanikaga, R.; Holzwarth, A. R.; Schaffner, K. *Angew. Chem., Int. Ed.* **1996**, *35*, 772−774.
(37) Grin, M. A.; Lonin, I. S.; Fedyunin, S. V.; Tsiprovskiy, A. G.; Strizhakov, A. A.; Tsygankov, A. A.; Krasnovsky, A. A.; Mironov, A. F. *Mendeleev Commun.* **2007**, *17*, 209−211.
(38) Muthiah, C.; Kee, H. L.; Diers, J. R.; Fan, D.; Ptaszek, M.; Bocian, D. F.; Holten, D.; Lindsey, J. S. *Photochem. Photobiol.* **2008**, *84*, 786−801.
(39) Kee, H. L.; Diers, R. J.; Ptaszek, M.; Muthiah, C.; Fan, D.; Bocian, D. F.; Lindsey, J. S.; Holten, D. *Photochem. Photobiol.* **2009**, *85*, 909−920.
(40) Taniguchi, M.; Ra, D.; Kirmaier, C.; Hindin, E.; Schwartz, J. K.; Diers, J. R.; Knox, R. S.; Bocian, D. F.; Lindsey, J. S.; Holten, D. *J. Am. Chem. Soc.* **2003**, *125*, 13461−13470.
(41) Birks, B. *Photophysics of Aromatic Molecules*; Wiley Interscience: New York, 1970.
(42) Wang, J.; Yang, E.; Diers, J. R.; Niedzwiedzki, D. M.; Kirmaier, C.; Bocian, D. F.; Lindsey, J. S.; Holten, D. *J. Phys. Chem. B* **2013**, *117*, 9288−9304.
(43) (a) Fortage, J.; Göransson, E.; Blart, E.; Becker, H.-C.; Hammarström, L.; Odobel, F. *Chem. Commun.* **2007**, 4629−4631. (b) Fortage, J.; Boixel, J.; Blart, E.; Hammarström, L.; Becker, H. C.; Odobel, F. *Chem.—Eur. J.* **2008**, *14*, 3467−3480. (c) Wielopolski, M.; Atienza, C.; Clark, T.; Guldi, D. M.; Martin, N. *Chem.—Eur. J.* **2008**, *14*, 6379−6390.
(44) Laha, J. K.; Muthiah, C.; Taniguchi, M.; McDowell, B.; Ptaszek, M.; Lindsey, J. S. *J. Org. Chem.* **2006**, *71*, 4092−4102.
(45) (a) Ka, J. W.; Lee, C. H. *Tetrahedron Lett.* **2000**, 4609−4613. (b) Maligaspe, E.; Tkachenko, N. V.; Subbaiyan, N. K.; Chitta, R.; Zandler, M. E.; Lemmetyinen, L.; D'Souza, F. *J. Phys. Chem. A* **2009**, *113*, 8478−8489.
(46) Ptaszek, M.; Bhaumik, J.; Kim, H.-J.; Taniguchi, M.; Lindsey, J. S. *Org. Process Res. Dev.* **2005**, *9*, 651−659.
(47) Yu, Z.; Ptaszek, M. *Org. Lett.* **2012**, *14*, 3708−3711.
(48) Krayer, M.; Ptaszek, M.; Kim, H.-J.; Meneely, K. R.; Fan, D.; Secor, K.; Lindsey, J. S. *J. Org. Chem.* **2010**, *75*, 1016−1039.
(49) For other examples of X-ray structures of bacteriochlorin, see ref 20 and: (a) Barkigia, K. M.; Fajer, J.; Chang, C. K.; Young, R. *J. Am. Chem. Soc.* **1984**, *106*, 6457−6459. (b) Barkigia, K. M.; Gottfried, D. S.; Boxer, S. G.; Fajer, J. *J. Am. Chem. Soc.* **1989**, *111*, 6444−6446. (c) Barkigiu, K. M.; Thompson, M. A.; Fajer, J. *Inorg. Chem.* **1991**, *30*, 2233−2236. (d) Ogikubo, J.; Meehan, E.; Engle, J. T.; Ziegler, C. J.; Brückner, C. *J. Org. Chem.* **2013**, *78*, 2840−2852. (e) Pandey, R. K.; Isaac, M.; MacDonald, I.; Medforth, C. J.; Senge, M. O.; Dougherty, T. J.; Smith, K. M. *J. Org. Chem.* **1997**, *62*, 1463−1472. (f) Samankumara, L. P.; Wells, S.; Zeller, M.; Acuña, A. M.; Röder, B.; Brückner, C. *Angew. Chem., Int. Ed.* **2012**, *51*, 5757−5760. (g) Samankumara, L. P.; Zeller, M.; Krause, J. A.; Brückner, C. *Org. Biomol. Chem.* **2010**, *8*, 1951−1965. (h) Vasudevan, J.; Stibrany, R. T.; Bumby, J.; Knapp, S.; Potenza, J. A.; Emge, T. J.; Schugar, H. J. *J. Am. Chem. Soc.* **1996**, *118*, 11676−11677.
(50) Kim, H.-J.; Lindsey, J. S. *J. Org. Chem.* **2005**, *70*, 5475−5486.
(51) Gust, D.; Moore, T. A.; Moore, A. L.; Leggett, L.; Lin, S.; DeGraziano, J. M.; Hermant, R. M.; Nicodem, D.; Craig, P.; Seely, G. R.; Nieman, R. A. *J. Phys. Chem.* **1993**, *97*, 7926−7931.
(52) (a) Christian, N. A.; Milone, M. C.; Ranka, S. S.; Li, G.; Frail, P. R.; Davis, K. P.; Bates, F. S.; Therien, M. J.; Ghoroghchian, P. P.; June, C. H.; Hammer, D. A. *Bioconjugate Chem.* **2007**, *18*, 31−40. (b) Ghorogchian, P. P.; Frail, P. R.; Susumu, K.; Park, T.-H.; Wu, S. P.; Uyeda, H. T.; Hammer, D. A.; Therien, M. J. *J. Am. Chem. Soc.* **2005**, *127*, 15388−15390. (c) Ghoroghchian, P. P.; Frail, P. R.; Susumu, K.; Blessington, D.; Brannan, A. K.; Bates, F. S.; Chance, B.; Hammer, D. A.; Therien, M. J. *Proc. Natl. Acad. Sci. U.S.A.* **2005**, *102*, 2922−2927. (d) Wu, S. P.; Lee, I.; Ghoroghchian, P.; Frail, P. R.; Zheng, G.; Glickson, J. D.; Therien, M. J. *Bioconjugate Chem.* **2005**, *16*, 542−550.
(53) Borbas, K. E.; Chandrashaker, V.; Muthiah, C.; Kee, H. L.; Holten, D.; Lindsey, J. S. *J. Org. Chem.* **2008**, *73*, 3145−3158.
(54) Reddy, K. R.; Lubian, E.; Pavan, M. P.; Kim, H.-J.; Yang, E.; Holten, D.; Lindsey, J. S. *New J. Chem.* **2013**, *37*, 1157−1173.